

## **NOTICE CONCERNING COPYRIGHT RESTRICTIONS**

This document may contain copyrighted materials. These materials have been made available for use in research, teaching, and private study, but may not be used for any commercial purpose. Users may not otherwise copy, reproduce, retransmit, distribute, publish, commercially exploit or otherwise transfer any material.

The copyright law of the United States (Title 17, United States Code) governs the making of photocopies or other reproductions of copyrighted material.

Under certain conditions specified in the law, libraries and archives are authorized to furnish a photocopy or other reproduction. One of these specific conditions is that the photocopy or reproduction is not to be "used for any purpose other than private study, scholarship, or research." If a user makes a request for, or later uses, a photocopy or reproduction for purposes in excess of "fair use," that user may be liable for copyright infringement.

This institution reserves the right to refuse to accept a copying order if, in its judgment, fulfillment of the order would involve violation of copyright law.

EVALUATION AND TARGETING OF GEOTHERMAL ENERGY RESOURCES  
IN THE SOUTHEASTERN UNITED STATES

Progress Report

John K. Costain, Lynn Glover III, and A. Krishna Sinha

Principal Investigators

April 1, 1977 - June 30, 1977

**NOTICE**  
This report was prepared as an account of work sponsored by the United States Government. Neither the United States nor the United States Department of Energy, nor any of their employees, nor any of their contractors, subcontractors, or their employees, makes any warranty, express or implied, or assumes any legal liability or responsibility for the accuracy, completeness or usefulness of any information, apparatus, product or process disclosed, or represents that its use would not infringe privately owned rights.

UNDER CONTRACT NO. EY-76-S-05-5103

PREPARED FOR THE ENERGY RESEARCH AND DEVELOPMENT ADMINISTRATION

Department of Geological Sciences  
Virginia Polytechnic Institute and State University  
Blacksburg, Virginia 24061

## **DISCLAIMER**

**This report was prepared as an account of work sponsored by an agency of the United States Government. Neither the United States Government nor any agency Thereof, nor any of their employees, makes any warranty, express or implied, or assumes any legal liability or responsibility for the accuracy, completeness, or usefulness of any information, apparatus, product, or process disclosed, or represents that its use would not infringe privately owned rights. Reference herein to any specific commercial product, process, or service by trade name, trademark, manufacturer, or otherwise does not necessarily constitute or imply its endorsement, recommendation, or favoring by the United States Government or any agency thereof. The views and opinions of authors expressed herein do not necessarily state or reflect those of the United States Government or any agency thereof.**

## **DISCLAIMER**

**Portions of this document may be illegible in electronic image products. Images are produced from the best available original document.**

TABLE OF CONTENTS

	<u>Page</u>
ABSTRACT . . . . .	2
RESEARCH OBJECTIVES. . . . .	5
INTRODUCTION . . . . .	7
PERSONNEL OF PROGRAM . . . . .	9
PROGRESS . . . . .	10
A. GEOLOGY . . . . .	A- 1
Operations . . . . .	A- 2
Petrography of the Win 1 Drill Core of the Rion Pluton. . . . .	A- 4
Winnsboro Plutonic Complex . . . . .	A-14
The Petersburg Batholith . . . . .	A-26
References . . . . .	A-42
B. GEOCHEMISTRY. . . . .	B- 1
Win 1 Core Samples . . . . .	B- 2
C. GEOPHYSICS. . . . .	C- 1
Geothermal Gradients and Heat Flow . . . . .	C- 2
Heat Generation. . . . .	C-11
Relationship Between Surface Heat Generation and Surface Heat Flow. . . . .	C-17
Partial Confirmation of Radiogenic Model . . . . .	C-23
Interpretation of Gravity Data . . . . .	C-27
References . . . . .	C-30
OVERVIEW AND SUMMARY . . . . .	11
COMPLIANCE WITH CONTRACT REQUIREMENTS. . . . .	12

## ABSTRACT

The objective of this research is to develop and apply targeting procedures for the evaluation of low-temperature radiogenically-derived geothermal resources in the eastern United States utilizing geological, geochemical, and geophysical data. Detailed study of the Winnsboro complex, South Carolina, is continuing as part of a broader project to provide insight into the behavior of uranium and thorium in syn- and post-metamorphic granitic plutons. In the area of the Winnsboro complex, a regional medium-pressure metamorphic event which reached amphibolite facies was followed by deformation and uplift with decrease in regional temperature and pressure. The Winnsboro complex was intruded with a resultant low-pressure contact metamorphism which reached hornblende hornfels grade in the xenoliths of the relatively dry Winnsboro biotite-hornblende granite and somewhat lower grade in xenoliths of the later, wetter Rion biotite granite.

In a continuing effort to develop a correlation between bulk chemistry and U and Th, the index  $\text{CaO}/(\text{K}_2\text{O} + \text{Na}_2\text{O})$  was applied to the core from the Rion pluton. A good negative correlation was found between this index and the uranium content of the core from the Rion pluton. There is a good positive correlation between U and  $\text{SiO}_2$  in the Rion core.

An excellent correlation between near-surface heat flow,  $q$ , and near-surface heat generation,  $A$ , was found for drill sites in the Winnsboro-Rion, Liberty Hill-Kershaw, and Roxboro plutons. These plutons span a distance of about 450 km and span an age of about 275 m.y. The equation of the straight-line relationship is  $q = 0.66 + 7.2 \times 10^{-5} A$ .

The slope is essentially the same as that found in New England; the intercept is slightly less than that for New England. The results imply that the gross geochemistry of the upper crust in the southeast is similar to that in New England, but that a local variation (increase) in heat flow from the upper mantle is present in New England. Transition zones between regions of different mantle heat flow are known to be relatively narrow in other areas where more heat flow data are available. The discovery and delineation of similar regions of anomalously high mantle heat flow in the southeast United States must therefore await a higher density of heat flow determinations.

The existence of the linear relationship in the southeast United States is encouraging, since it strengthens the capability for prediction of subsurface temperatures based on a radiogenic model. Partial confirmation of a radiogenic model has been provided by a geothermal gradient of  $37.4^{\circ}\text{C}/\text{Km}$  ( $2^{\circ}\text{F}/100\text{ ft.}$ ) in an existing hole in sediments of the Atlantic Coastal Plain at Stumpy Point, North Carolina. The bottomhole temperature at a depth of 1.35 km (4430 ft.) is  $66^{\circ}\text{C}$  ( $150^{\circ}\text{F}$ ). The gradient is consistent with theoretical predictions using reasonable values of thermal conductivity and heat generation in a buried radiogenic source. The site is on the flank of a large negative Bouguer gravity anomaly.

## RESEARCH OBJECTIVES

The objective of this research is to develop and apply targeting procedures for the evaluation of low-temperature radiogenically-derived geothermal resources in the eastern United States utilizing geological, geochemical, and geophysical data.

The optimum sites for geothermal development in the tectonically stable eastern United States will probably be associated with areas of relatively high heat flow derived from crustal igneous rocks containing relatively high concentrations of radiogenic heat-producing elements. The storage of commercially-exploitable geothermal heat at accessible depths (1-3 km) will also require favorable reservoir conditions in rocks overlying a radiogenic heat source. In order to systematically locate these sites, a methodology employing geological, geochemical, and geophysical prospecting techniques is being developed and applied. The radiogenic distribution within the igneous rocks of various ages and magma types will be determined by a correlation between radioelement composition and the rock's bulk chemistry. Surface sampling and measurements of the radiogenic heat-producing elements are known to be unreliable as they are preferentially removed by ground water, circulation, and weathering. The correlation between the bulk chemistry of the rock (which can be measured reliably from surface samples) and radiogenic heat production is being calibrated by detailed studies at a number of locations in the eastern United States.

Initial studies will develop a methodology for locating radiogenic heat sources buried beneath the insulating sedimentary rocks of the



Coastal Plain of South Carolina, North Carolina, and Virginia. Additional heat flow and thermal gradient measurements are being made in available deep wells.

## INTRODUCTION

Detailed study of the Winnsboro complex, South Carolina, is continuing as part of a broader project to provide insight to the behavior of uranium and thorium in syn- and post-metamorphic granitic plutons during periods of crystallization, deuteric alteration, and weathering. In following sections of this report, we present chemical and geophysical data for the Win 1 core from the Rion pluton of the Winnsboro complex. Win 1 petrography is described at the beginning of this section.

The results of a study of xenoliths and contact aureole of the Winnsboro complex are presented in this section. The study was made to determine the regional metamorphic grade of the country rocks, the structural relations of the Winnsboro plutons to the country rocks, the sequence of intrusion (later phases tend to be higher in uranium), and the emplacement temperatures and pressures of the Winnsboro plutons. These characteristics of the Winnsboro complex will be compared to those of the Liberty Hill pluton (Speer, VPI&SU-5103-3, and research in progress), which was emplaced under similar conditions, but in a lower grade (greenschist facies) terrain.

With this type of approach, observed uranium and thorium distributions in these and other plutons may be used as predictive models for unstudied areas. The possibility of relating some of these geological parameters to gravity and magnetic models will also have application to prediction of basement geology (heat sources) under the Atlantic Coastal Plain.

Preliminary work on the Petersburg, Virginia batholith indicates that it was emplaced late in the metamorphic history of the eastern

Piedmont at about 300 m.y. ago. Slightly younger deformation is shown by local low-grade mylonitic zones and associated folds. At approximately 220 m.y. ago, dilational fracturing occurred under zeolite facies conditions.

The linear relationship between heat flow and heat generation found for the southeast United States implies regional equilibration of  $U$  and  $Th$  on a large scale. If the relationship continues to be upheld as additional data become available, our capability for the prediction of deep subsurface temperatures by drilling shallow to intermediate depth holes will be strengthened.

PERSONNEL OF PROGRAM

(April 1 - June 30, 1977)

GEOLOGY AND PETROLOGY, Lynn Glover III, Principal Investigator

J. A. Speer, Research Associate  
S. S. Farrar, Research Associate  
S. W. Becker, Research Associate  
A. R. Bobyarchick, Research Associate (part time)  
A. Baldasari, Laboratory Aide

GEOCHEMISTRY, A. Krishna Sinha, Principal Investigator

B. A. Merz, Research Associate  
S. Dickerson, Laboratory Aide  
S. Higgins (part-time Lab Aide)  
M. Lipford (part-time Lab Aide)

GEOPHYSICS, J. K. Costain, Principal Investigator

C. S. Rohrer, Research Specialist (resigned 6-30-77)  
L. D. Perry, Research Associate  
J. A. Dunbar (part time)

Administrative Assistant, Patricia C. Sullivan

Secretary, Margie Strickler

Drillers

W. G. Coulson, Core Driller  
R. G. Gravley, Driller Helper

PROGRESS

## OVERVIEW AND SUMMARY

Detailed study of the Winnsboro complex, South Carolina, has continued as part of a broader project to provide insight into the behavior of uranium and thorium in syn- and post-metamorphic granitic plutons during emplacement. A systematic distribution of uranium and thorium is indicated by the remarkable linear correlation between heat flow and heat production for the three sites described in this report. This implies equilibration of uranium and thorium on a regional scale of heretofore unsuspected dimensions. Since the slope of the straight-line relationship is the same as that for New England, it can be inferred that the gross geochemical properties of the crust in the southeast are similar to those in the northeast United States. The intercept of the straight-line relationship is slightly different in New England. The reason for the difference may be due to relatively "local" differences in the heat flow from the lower crust and/or mantle in New England. In other areas in the United States, transitions between regions of different upper mantle heat flow are relatively sharp. Hence, as more heat flow data become available to construct "reduced heat flow" maps, the probability of the discovery and delineation of similar anomalous areas in the southeast United States increases.

Our results to date suggest that the linear relationship between heat flow and heat generation will be an important component of a general targeting procedure for the prediction of subsurface temperatures in the sediments of the Atlantic Coastal Plain.

COMPLIANCE WITH CONTRACTUAL REQUIREMENTS

Principal investigators John K. Costain, Lynn Glover III, and A. K. Sinha, in accordance with Article A-I of Appendix A to the here-  
inmentioned contract, have devoted five weeks, one month, and one-half  
month, respectively, of their efforts to performance under the contract.  
They plan to devote 10 weeks, four weeks, and 10 weeks, respectively,  
to the contract during the next three-month report period.

All contract requirements have been complied with.

*John K Costain*  
\_\_\_\_\_  
John K. Costain

*A. K. Sinha JKC*  
\_\_\_\_\_  
A. K. Sinha

*Lynn Glover III*  
\_\_\_\_\_  
Lynn Glover III

A. GEOLOGY

Lynn Glover III, Principal Investigator

J. A. Speer, Research Associate

S. S. Farrar, Research Associate

S. W. Becker, Research Associate

A. Baldasari, Laboratory Aide



## Operations

During the period March 1 to June 30, 1977, 15-1/2 man-weeks were spent conducting field work. Detailed mapping of the country rocks surrounding the Rolesville batholith was continued, and mapping of the Liberty Hill and Winnsboro plutonic complexes was completed. Field work was also begun on the Petersburg granite and its geologic setting. Locations of the field areas are indicated on Figure A1. Further reconnaissance studies were made of granitic and gabbroic plutons and their contact aureoles in North and South Carolina and Georgia. In addition, sites for four drill holes were located in the Rolesville batholith.

Drilling operations during this period involved three drill holes. Roxboro 3, the third hole in the Roxboro granite, was completed at 694 ft. (212 m); a hole (SB-1) in the slate belt volcanic rocks east of the Roxboro granite also reached 694 ft. (212 m). The first hole in the Rolesville batholith was drilled in the Castalia pluton to a depth of 691 ft. (211 m).

Samples collected during this reporting period comprise the following:

	<u>Chemistry and Heat Production Samples</u>	<u>Total Samples</u>
Liberty Hill, SC surface	2	29
Winnsboro, SC surface	4	38
Win 1 (1884')	16	17
Rolesville, NC surface	-	25
Ro1 1 (691')	-	-
Roxboro, NC surface	-	-
Rox 1 (884')	-	-
Rox 2 (702')	-	-
Rox 3 (694')	-	-
Slate Belt, NC SB 1 (694')	-	-
Petersburg, VA surface	33	58

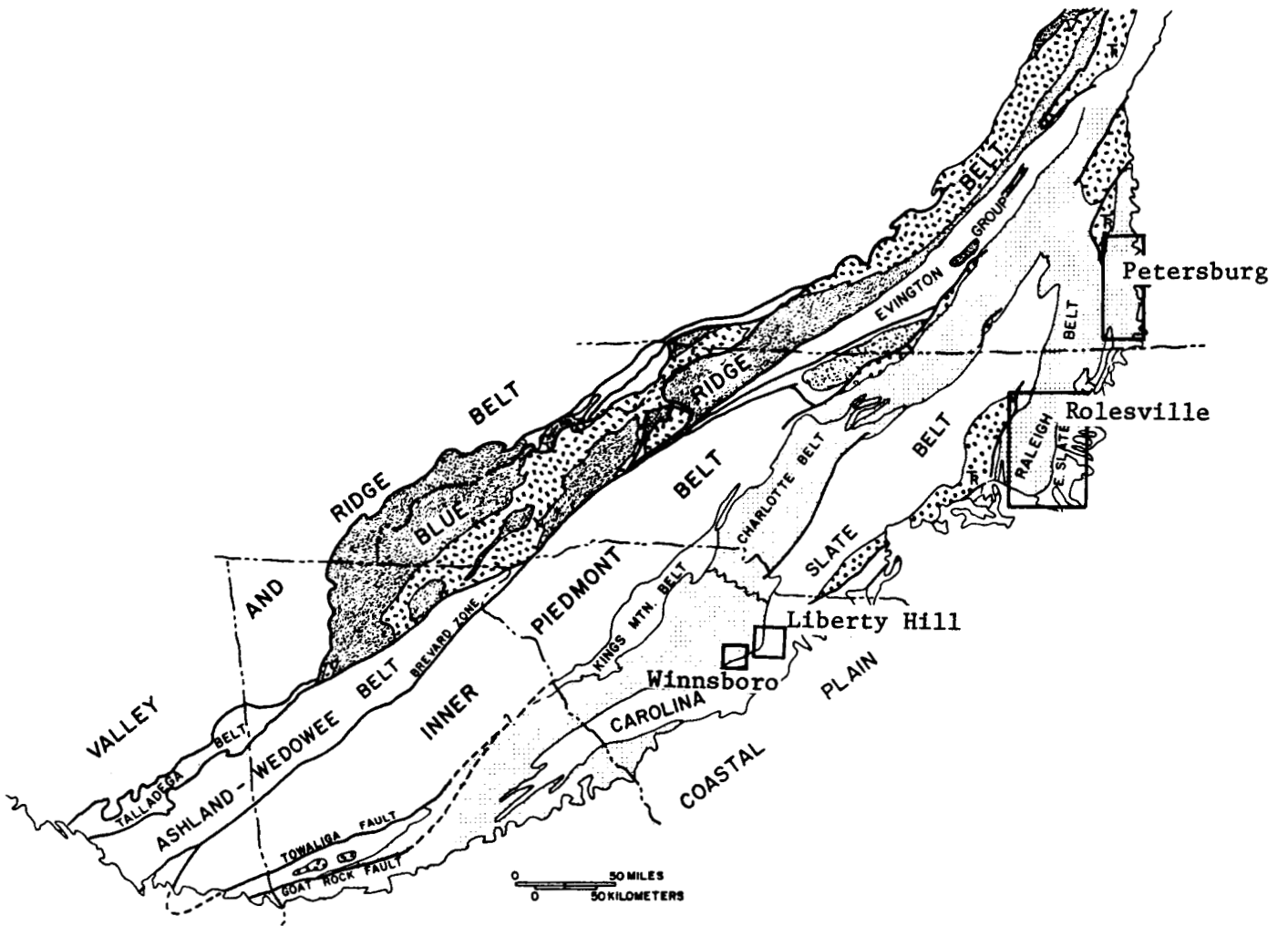


FIGURE A1 GENERALIZED GEOLOGY OF THE SOUTHERN APPALACHIANS  
 [MODIFIED BY L. GLOVER III FROM FISHER & OTHERS(1970)]

## Petrography of the Win 1 Drill Core of the Rion Pluton

Stewart Farrar

An 1884 ft. (575 m) core, Win 1, has been taken from the east-central part of the Rion pluton of the Winnsboro complex (Fig. A2). This core is from the medium-grained Rion granite, which has been previously described from surface samples in report VPI&SU-5103-2. Figure A3 is a combined lithologic and gamma log of Win 1. Sample locations for petrography, chemistry, and heat generation are shown on this log.

The granite is petrographically uniform for large segments of the core. It is generally hypidiomorphic-granular with microperthitic microcline slightly larger (0.5-0.8 cm length) than the other minerals. Less commonly, the microcline is as large as 1.0 to 1.2 cm and is distinctly coarser than the other minerals. The minerals rarely have a preferred orientation, but uncommon, fine-grained layers have a gently-dipping, weak biotite foliation. From 980 to 1100 ft. (300-335 m) and from 1665 to 1775 ft. (507-541 m), the granite is layered. The layers vary from 0.3 to 3 m thick and have sharp to diffuse contacts. Variation of biotite content from about 3 to 6 percent is the most visible change, but there is also some variation in grain size, with leucocratic layers usually a little coarser than biotite-rich layers. Layered areas commonly also have small biotite-rich xenoliths.

Mineralogy of the granite is the same throughout the core: microperthitic microcline, oligoclase (moderately zoned,  $An_{22-17}$  with albite rims), quartz, and biotite. Accessory minerals include opaques, zircon, titanite, allanite, and apatite. Deuteric reactions include partial alteration of biotite to chlorite, and moderate to strong saussuritization

of plagioclase (especially cores of grains) to epidote + muscovite + calcite.

Modes of Win 1 samples (Table A1) have approximately the same range as those from the Rion surface samples (Figs. A4 and A5). The apparently higher quartz content of the core samples is probably a result of counting the core samples in thin section, where fine-grained quartz is more easily recognized than in the stained slabs which were point counted for most of the surface samples.

There are two types of xenoliths in the Win 1 core. One type, comprised of biotite-rich layers (1-10 cm thick) with diffuse boundaries, is quite common. The mineralogy of this type is the same as the granite, but it has 20-25 percent biotite, the difference being made up in the lower modal amounts of microcline. The second type, a complex xenolith about 0.4 m thick, was encountered at 994 ft. (303 m). The outer, dominant phase, a fine-grained aplitic rock, contains minor biotite, some microcline, and is dominantly oligoclase + quartz. Both the plagioclase and the microcline grains have large rims with numerous fine-grained quartz inclusions. It appears that the surrounding granite was metasomatizing the quartz-rich xenolith. The inner, minor phase of this xenolith consists of two biotite-muscovite-rich clots, each of which is 2-3 cm in diameter. They are at least 60 percent biotite and contain muscovite, plagioclase, quartz, and opaque minerals. Each of the clots contains a healed fracture filled by an unidentified mineral which has caused a continuous strip of radiation damage in the bordering biotite. This complex xenolith, and the adjacent granite, give a positive spike on the gamma log. The granite sample from

Explanation

Rion pluton



rf - fine-medium grained biotite monzogranite.  
rm - medium-grained biotite monzogranite.



Border zone of Rion biotite monzogranite with plentiful country rock xenoliths.

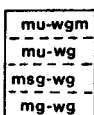
Winnsboro pluton



Coarse-grained biotite-hornblende granite, quartzsyenite, and quartz monzonite. C.I. < 10.



Medium- to coarse-grained, biotite-hornblende monzogranite. C.I. > 10.



Intimate mixture of small bodies of the Winnsboro granites with the indicated rock type described below.



Dutchmans Creek gabbro-norite.



Interlayered biotite and biotite-hornblende granitic gneiss; amphibolite; biotite schist; and migmatitic gneisses.



Metapelites, including muscovite-biotite-quartz feldspar gneisses; muscovite-sillimanite quartzite; quartz-muscovite-sillimanite schist; minor amphibolite; and hornfels derivatives of these units.



Biotite and biotite-hornblende granitic gneisses; leucogneisses; and minor amphibolite.



Muscovite schist; muscovite quartzite; and fine-grained quartzofeldspathic gneisses.



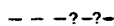
vg1 - amphibolite; biotite granitic gneiss.  
vg2 - amphibolite; biotite granitic gneiss; metamorphosed ultramafic rock.



Amphibole-plagioclase amphibolite; albite-epidote-chlorite greenstone; and fine-grained quartzofeldspathic gneisses.



Muscovite-biotite and chlorite phyllite; greenstone; and fine-grained quartzofeldspathic gneisses.



Contacts, queried where speculative.



Boundary of Winnsboro complex.



Strike and dip of S<sub>0</sub> and S<sub>1</sub> foliation.



Strike and dip of S<sub>2</sub> foliation.



Trend and plunge of F<sub>1</sub> hinge line.



Trend and plunge of F<sub>2</sub> hinge line.



Sample locality.

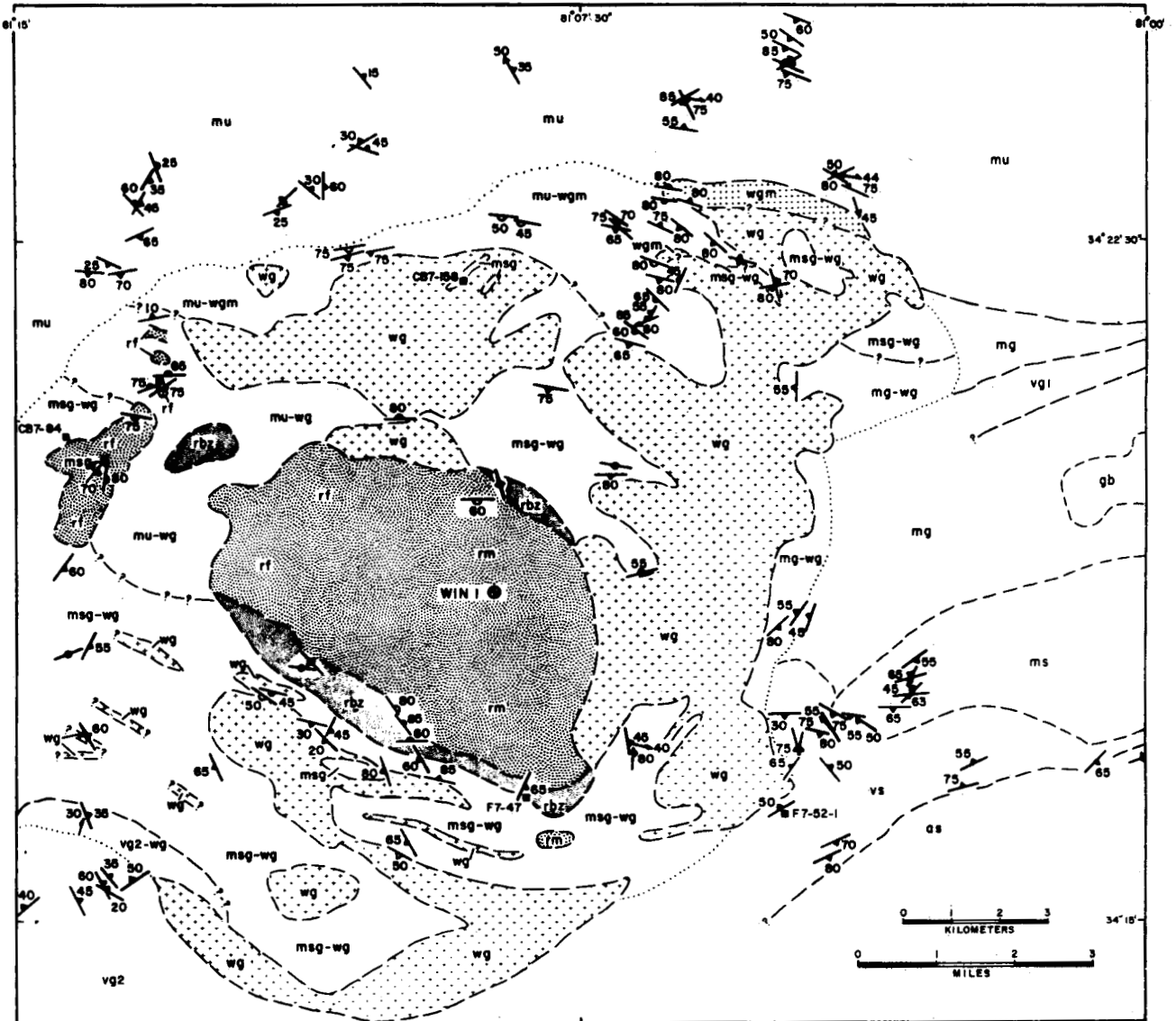


Figure A2. Geologic map of the Winnsboro plutonic complex, South Carolina.

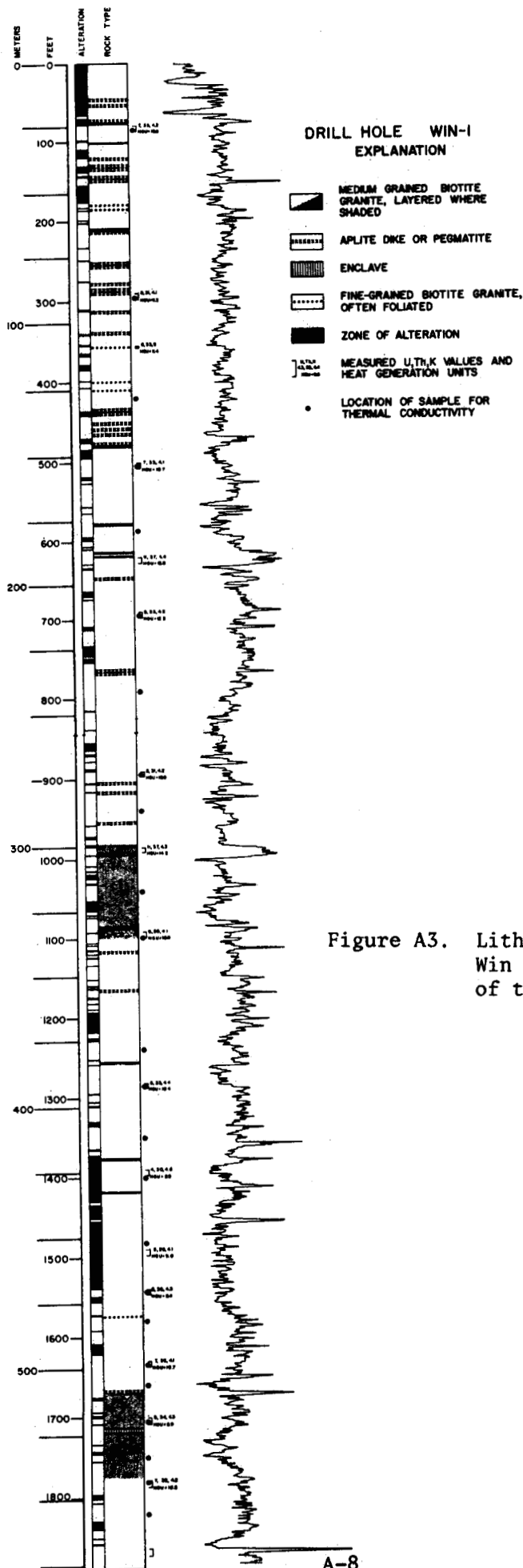


Figure A3. Lithologic and gamma log of the Win 1 core from the Rion pluton of the Winnsboro complex.

Table A1. Modal<sup>1</sup> data for Win 1 core samples.

Depth in meters	Sample number = Depth in feet	K-feldspar	Plagioclase	Quartz	Biotite	Accessories <sup>2</sup>
24.4	80	35.2	30.0	31.5	3.2	.3
88.4	290	28.5	32.6	32.3	5.4	1.2
108.5	356	39.7	27.7	28.5	3.7	.5
152.4	500	31.4	26.1	38.3	3.9	.3
189.0	620	42.4	24.5	30.2	2.7	.3
210.3	690	28.6	35.3	31.0	4.3	.9
271.3	890	31.6	35.6	28.4	4.0	.4
300.8	987	44.2	26.3	25.6	3.7	.2
332.8	1092	34.3	26.6	32.0	6.3	.8
390.5	1281	41.0	28.1	27.5	3.1	.3
469.4	1540	32.7	33.2	28.4	5.3	.4
496.8	1630	29.5	29.5	34.9	5.6	.5
518.5	1701	35.9	32.4	26.0	4.6	1.2
542.2	1779	30.8	30.8	32.8	5.2	.5
568.5	1865	39.7	26.1	28.9	4.9	.4

<sup>1</sup>Each mode is determined from 1000 points in one thin section.

<sup>2</sup>Accessories include opaque, titanite, apatite, zircon, allanite.



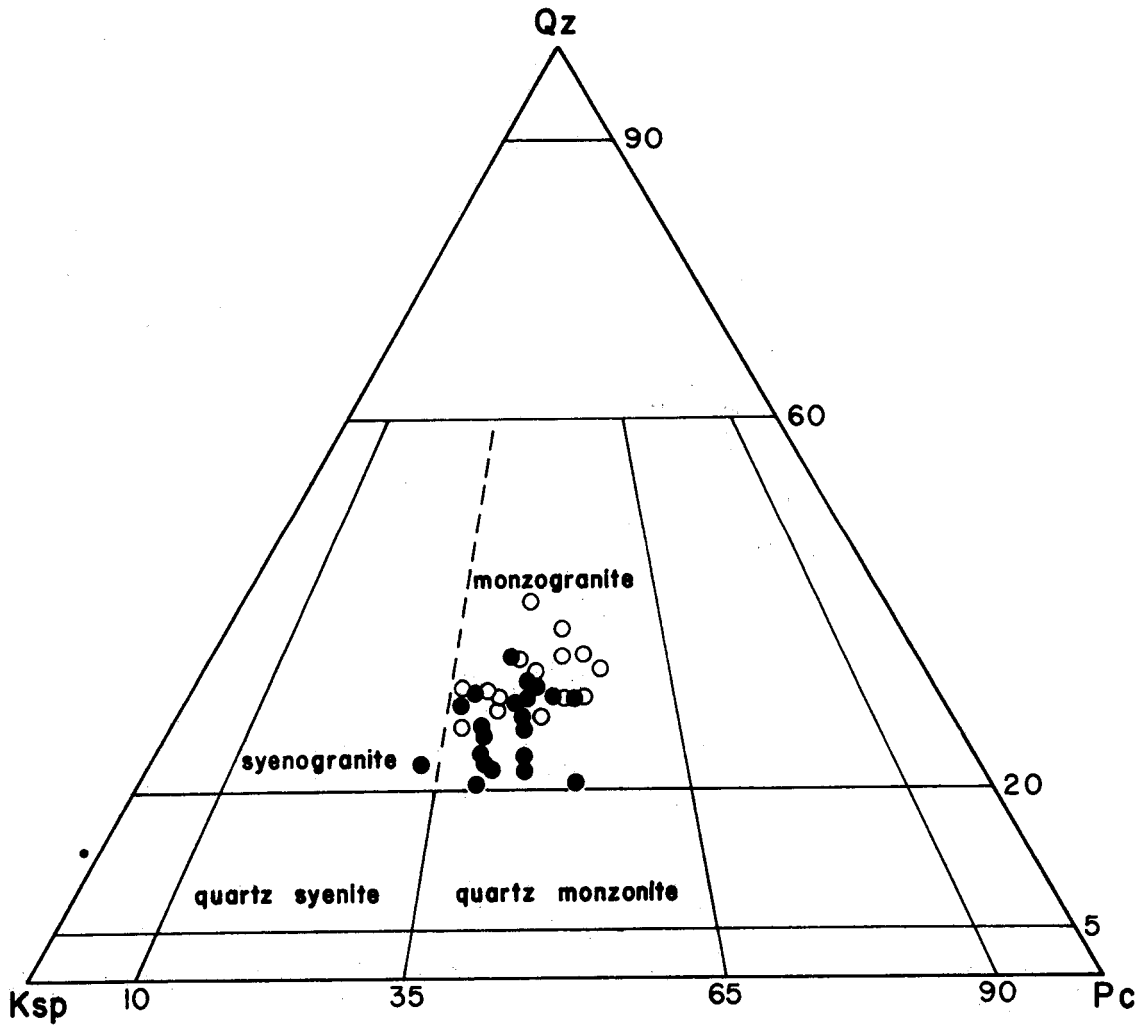


Figure A4. Triangular diagram of modal volume percent of alkali feldspar (Ksp), plagioclase (Pc), and quartz (Qz) for samples from the Win 1 core of the Rion pluton (O), and surface samples of the Rion pluton (●).

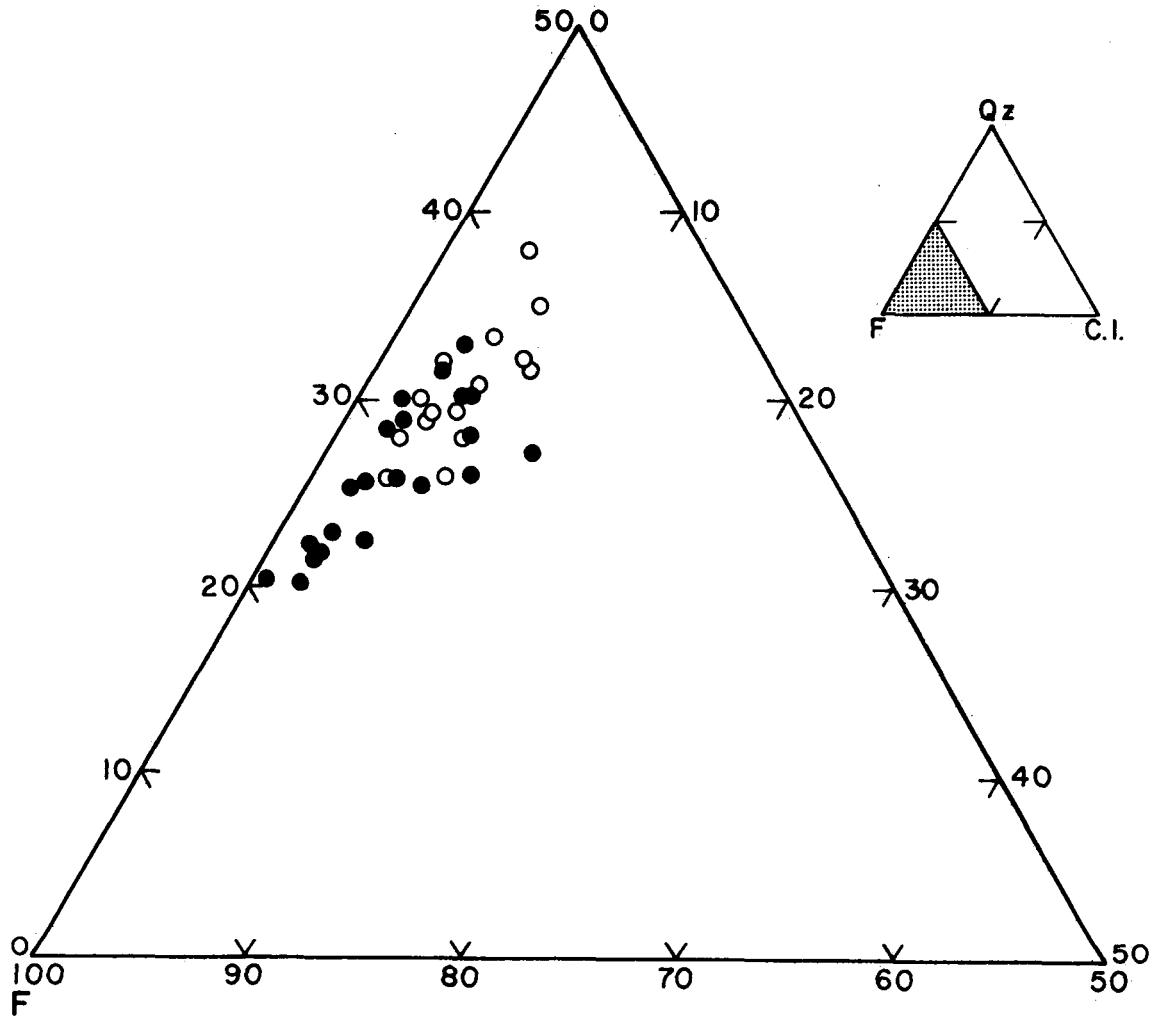


Figure A5. Triangular diagram of modal volume percent of total feldspar (F), quartz (Qz), and color index (C.I.) for samples from the Win 1 core of the Rion pluton (O), and surface samples of the Rion pluton (●).

this positive spike (987/993) has the highest heat production found in the Rion pluton.

There are several aplite dikes and numerous quartz-feldspar pegmatitic dikes intersected by the Win 1 core. The largest aplite dike (at 1117 ft. (340 m)) is 0.35 m thick and has a positive spike on the gamma log. Other aplite dikes and all quartz-feldspar pegmatitic dikes are 1-5 cm thick and are exaggerated in order to be shown on the lithologic log (Fig. A3). Some of these dikes give spikes on the gamma log and some have no recorded effect.

There are two major types of alteration of the Win 1 core. The core shows effects of surface weathering to approximately 25 m, and along fractures it is quite weathered and crumbly to approximately 60 m. Below 60 m altered core is essentially always associated with discrete fractures. These fractures normally contain pyrite, often with muscovite. Some fractures contain quartz, with or without accessory molybdenite (report VPI&SU-5103-3, p. A17). Many of the fractures are nearly vertical and run through the core for more than a meter. A few horizontal to moderately-dipping fractures contain calcite and zeolites.

Alteration of the granite around the fractures includes nearly complete reaction of plagioclase to muscovite + calcite + epidote. Biotite is completely altered to chlorite + opaque minerals. Microcline appears fresh in thin section, but in hand specimen it has a distinctly pink color near fractures and is light grey away from them. Two of the samples (1390/1396 and 1490/1496) taken for chemistry and heat generation are from core containing multiple steeply-dipping fractures with minor pyrite, and associated altered granite. These two samples give the two lowest heat

generation values measured in this core. Probably some of the uranium has been removed by solution along these fractures.

## Winnsboro Plutonic Complex

Stewart Farrar

### Introduction

The Winnsboro complex is composed of two plutons and the included contact metamorphosed country rock within the boundary shown in Figure A2. The Rion pluton, a medium-grained biotite monzogranite, constitutes the central portion of the complex. The Winnsboro pluton, composed of medium- to coarse-grained biotite-hornblende granite, quartz syenite, and quartz monzonite, occurs as a series of lenticular bodies surrounding the Rion monzogranite.

The plutons of the Winnsboro complex were emplaced within the edge of the Charlotte belt, a sequence of amphibolite grade metamorphic rocks of sedimentary, volcanic, and plutonic origin. Along its southern border, the Winnsboro pluton is in contact with the dominantly greenschist facies rocks of the Carolina slate belt. These rocks are of sedimentary and volcanic origin.

Petrographic and modal analyses of both the Rion and Winnsboro plutons were presented in report VPI&SU-5103-2. In addition, elsewhere in this report, an 1884 ft. (575 m) core from the Rion pluton is described.

This report concentrates on the relationship of the Winnsboro complex to surrounding metamorphic rocks. It briefly discusses stratigraphy, structure, regional metamorphism, and contact metamorphism in the immediate vicinity of the Winnsboro complex.

## Charlotte Belt and Carolina Slate Belt Stratigraphy

In this section, rock types of the Charlotte belt and Carolina slate belt in the vicinity of the Winnsboro complex are briefly described. This study covers the same area as that of Wagener (1970, 1973). Because this study has concentrated on structure and contact metamorphism and ignored some areas examined by Wagener, the reader is referred to Wagener (1970, 1973) for more complete descriptions of some rock units. Abbreviations refer to map units in Figure A2, and in Wagener (1970).

### Undifferentiated gneisses (mu)

This composite unit consists of: (1) thin-layered biotite, and biotite-hornblende granitic gneisses; (2) biotite-hornblende-plagioclase amphibolite; (3) biotite schist; and (4) migmatitic gneisses, some of which are very leucocratic, and all of which appear to be foliated. Wagener (1970) divided this unit into his ag, vg, and mu units. Examination of roadcuts and gravel pits (some of which are new since Wagener's mapping) indicates that these units cannot be differentiated as described by Wagener. Migmatitic leucogranitic gneisses increase in abundance to the west, but all of the interlayered rock types continue across the mapped area of this unit.

### Pelitic gneisses (msg)

This unit includes biotite-quartz-feldspar gneisses, muscovite-sillimanite quartzite, quartz-muscovite-sillimanite schist, minor hornblende-plagioclase gneiss and amphibolite, and hornfels derivatives of

these rock types. This unit comprises Wagener's mf unit and part of his ms unit. Dominated by pelitic compositions which have developed hornfels mineral assemblages in the Winnsboro complex, these rocks are discussed in the metamorphic section.

#### Biotite and hornblende gneisses (mg)

Biotite and hornblende quartzofeldspathic gneisses, biotite-quartz-feldspar leucogneiss, and minor hornblende-plagioclase amphibolite make up this unit which was described by Wagener (1970), but was not examined in this study.

#### Muscovite schist (ms)

This unit includes muscovite schist, muscovite-quartzite, and fine-grained quartzofeldspathic gneisses. This is a unit from Wagener (1970) which has been retained in the southeastern part of the map area where no  $Al_2SiO_5$  minerals have been found. Within the Winnsboro complex, sillimanite has been found in areas mapped by Wagener as muscovite schist. These areas have been included in the pelitic gneiss unit.

#### Amphibolite (vg1/vg2)

The vg1 map unit is comprised of hornblende-plagioclase amphibolite interlayered with biotite-quartz feldspar granitic gneiss. This is a unit from Wagener (1970). Where amphibolite is clearly subordinate to the quartzofeldspathic gneiss, this unit has been included in the undifferentiated gneiss unit (mu). Unit vg2, in the southwestern corner of

the mapped area, is similar to vg2, but also includes outcrops of a metamorphosed ultramafic rock, the extent of which is unknown.

#### Amphibolite-greenstone (vs)

Fine-grained amphibole-plagioclase amphibolite, albite-epidote-chlorite greenstone and fine-grained quartzofeldspathic gneisses make up this unit which lies close to the amphibolite facies-greenschist facies boundary. This unit has been subjected to contact metamorphism where it lies near the Winnsboro granite. Contacts are essentially those of Wagener (1970).

#### Phyllite (as)

Muscovite-biotite and chlorite phyllite, greenstone, and fine-grained quartzofeldspathic gneisses make up this unit. Shown as mapped by Wagener (1970), this unit and the amphibolite-greenstone unit lie in a traverse to be discussed in a future report.

#### Gabbro-norite (gb)

The Dutchmans Creek gabbro-norite is a post-tectonic intrusive which was not examined for this report. The contact is from Wagener (1970).

### Structure

#### Charlotte belt

Lithologic layering ( $S_0$ ) in the Charlotte belt rocks, which surround most of the Winnsboro complex, is parallel, on the macroscopic scale, to



a strong  $S_1$  foliation.  $S_1$  is defined by the preferred orientation of minerals, and in some cases by a younger, weak layering of mafic minerals (usually biotite and hornblende).  $S_0$  and  $S_1$  in these Charlotte belt rocks have been found to diverge only in the hinge areas of small mesoscopic  $F_1$  folds. On the regional scale,  $S_0$  appears to parallel  $S_1$ , and it has not been possible to define any major  $F_1$  folds at this time. The combined  $S_0 + S_1$  foliation is the most commonly measured foliation in these Charlotte belt rocks.

The combined  $S_0 + S_1$  foliation has been folded into moderate to tight  $F_2$  folds. On the regional scale, Overstreet and Bell (1965) show that the Charlotte belt rocks of the Winnsboro area lie in the core of a major fold which has a northeast-striking axial surface. This fold is interpreted, in this study, to be a major  $F_2$  fold. Small, mesoscopic,  $F_2$  folds are found at a number of locations in Charlotte belt lithologies. The axial surfaces of these  $F_2$  folds are defined by a crenulation foliation ( $S_2$ ) in micaceous rocks. In other lithologies  $S_2$  has not developed.

To the east of the Winnsboro complex, outside the influence of the granitic plutons, the  $S_0 + S_1$  foliation broadly conforms to the shape of the macroscopic  $F_2$  fold (Fig. A2). Measurements of  $S_2$  northeast of the complex have a consistent attitude of approximately N65E, 75S. Mesoscopic  $F_2$  folds in this area are also consistent in their asymmetry, with an S-shape, indicating closure of the macroscopic  $F_2$  fold is to the northeast. Hinge lines of these mesoscopic  $F_2$  folds plunge approximately 45, S80E, suggesting, but not proving, that the macroscopic fold is somewhat overturned to the northwest, rather than upright, as is indicated by Overstreet and Bell (1965).  $S_2$  measurements southeast of the Winnsboro

complex have a similar northeast trend, but the relations in this area are complicated by the presence of a possible major, northeast-trending ductile deformation zone (this zone will be discussed in a future report). Structural trends northwest of the Winnsboro complex are somewhat random, probably, in large part, as a result of the migmatization of the granitic gneisses during regional metamorphism, which appears to have been coeval with  $S_1$ .

#### Structure of the Winnsboro complex

The Winnsboro complex has an approximately elliptical shape (dotted line, Fig. A2), although it may expand again to the west, beyond the limit of the mapped area. Within the complex, structural attitudes have been modified by the post-tectonic intrusions of the Winnsboro and Rion plutons. In Figure A2, only the large, relatively inclusion-free bodies of Winnsboro granite are shown. Charlotte belt country rock within the complex is in the form of large and small xenoliths and probable protrusions from the floor of the complex. These country rocks are mixed with an approximately equal volume of Winnsboro granite in the form of small xenolith-filled bodies. Most of the xenoliths are derived from strongly layered rocks and have a plate-like shape which lends itself to preferred orientation within the granite. The result, as seen in Figure A2, is the approximate conformity of  $S_0 + S_1$  of these xenoliths to the elliptical form of the complex. Measurements of the attitudes of xenoliths and the relatively rare flow foliation of the Winnsboro granite give a steeply inward-dipping conical shape for the complex.

The center of the complex is occupied by the Rion pluton. Although the interior of the Rion pluton is essentially free of flow foliation and has only small rounded xenoliths, the outer border zone (rbz, Fig. A2) has numerous xenoliths, the orientations of which also support the conical shape of the complex. That this conical shape postdates the formation of the  $S_2$  foliation in the country rock is best illustrated by the reoriented  $S_2$  foliation within the boundary of the complex. This is illustrated in the large area of mixed country rock and Winnsboro granite in the northeastern part of the complex (Fig. A2).

### Metamorphism

#### Regional metamorphism

East of the Winnsboro complex, regional metamorphic grade increases from greenschist to amphibolite facies in a south to north traverse (Wagner, 1970). This increase in grade and accompanying changes in style of deformation define a gradational change from Carolina slate belt to Charlotte belt rocks in this area. Charlotte belt rocks (granitic gneisses and amphibolite) north of the Winnsboro complex are not obviously sensitive indicators of metamorphic grade, and increase or decrease in grade to the north has not been determined.

Within the Winnsboro complex, regional amphibolite facies conditions are indicated by the presence of sillimanite. It occurs in sillimanite-muscovite quartzite and sillimanite-quartz-muscovite schist (unit msg, Fig. A2). The prismatic sillimanite generally lies in the  $S_1$  foliation. Although it could possibly be pseudomorphic after muscovite, the sillimanite

appears to have grown during the regional metamorphic event, and thus predates the Winnsboro plutonic complex. No sillimanite has been found in the major muscovite schist unit (ms, Fig. A2) east of the Winnsboro complex, suggesting a decrease in metamorphic grade eastward. This agrees well with the structural interpretation (structure section) that the Winnsboro complex lies in the core of a major  $F_2$  fold which has folded the regional isograds to form a protrusion of the higher grade Charlotte belt rocks into the lower grade Carolina slate belt rocks.

The regionally developed aluminosilicate mineral found in most pelitic rocks of the southeastern Piedmont of South Carolina is kyanite--e.g., at the Lake Murray Spillway 20 km south of the Winnsboro complex (Secor and Wagener, 1968), and at Little Mountain 15 km southwest of the Winnsboro complex (Espenshade and Potter, 1960). Butler (1966), however, found kyanite in some areas, and sillimanite in other areas in York County, about 40 km north of the Winnsboro complex. Although Overstreet et al. (1960) reported muscovite pseudomorphic after kyanite at two localities within the Winnsboro complex, such clearly defined pseudomorphs have not been found in this study. This study has confirmed the presence of sillimanite as reported by Wagener (1970), and although some of this may be pseudomorphic after kyanite, no kyanite has been found in the vicinity of the Winnsboro complex.

The crystallization of well-developed sillimanite required a minimum temperature in the vicinity of 600°C and a probable pressure in the range 4-6 kb (Richardson et al., 1969). It is reasonable to assume that migmatite found in the granitic gneisses north of the Winnsboro complex formed during this period of maximum regional metamorphism. Small

leucogranitic bodies, apparently derived by partial melting of the gneisses, have a metamorphic fabric ( $S_1$ ) which clearly differentiates them from the later, post-tectonic granites of the Winnsboro complex. The evidence of partial melting suggests the temperature of this metamorphic event was probably somewhat higher than the minimum 600°C required by the sillimanite.

The regional metamorphic facies series for the eastern South Carolina Piedmont, as indicated by the regional development of kyanite and sillimanite, is the medium-pressure type of Miyashiro (1973).

#### Contact metamorphism

Contact metamorphism by the Winnsboro plutonic complex caused recrystallization of xenoliths and produced a contact aureole in the surrounding rocks. The areal extent of the contact aureole is not known, but it extends at least 0.5 km beyond the known limit of the Winnsboro pluton in a southeasterly direction (location F7-52-1, Fig. A2). It probably extends at least this far from the Winnsboro complex in other directions also. The width of the aureole is presently being investigated.

Texturally and mineralogically, the contact metamorphism has had the greatest effect on the pelitic gneisses, resulting in the conversion of these gneisses to relatively coarse-grained hornfels. Contact metamorphic effects on the granitic and amphibolitic gneisses are very difficult to differentiate from regional metamorphic effects. Examination of the contact aureole has, therefore, concentrated on pelitic rocks (unit msg, ms, and as, Fig. A2).

Hornfels assemblages in xenoliths and country rock lenses within the coarse-grained, biotite-hornblende granite of the Winnsboro pluton include combinations of the following minerals: muscovite, biotite, fibrolitic sillimanite, cordierite, andalusite, garnet, plagioclase, microcline, and quartz. Where quartz is absent or very limited, spinel and corundum have been found.

The highest grade assemblages in xenoliths of the coarse-grained Winnsboro pluton are characteristic of the hornblende hornfels facies:

- 1) garnet-cordierite-biotite-plagioclase-quartz (CB7-158, Fig. A2), and
- 2) garnet-cordierite-biotite-fibrolite-andalusite-quartz (CB7-84, Fig. A2).

One sample from the contact aureole of the coarse-grained Winnsboro pluton suggests a decrease in temperature to the muscovite hornfels facies with the assemblage:

cordierite-biotite-muscovite-fibrolite-andalusite-quartz  
(F7-52-1, Fig. A2).

Most evidence of lower grade contact metamorphism in the aureole is apparently disguised by previously existing regional amphibolite grade assemblages.

The contact metamorphic assemblages containing andalusite indicate that regional temperature and pressure had decreased significantly between the period of regional metamorphism, with crystallization of coarsely crystalline sillimanite, and the time of intrusion of the Winnsboro pluton

( $301 \pm 4$  m.y., Fullagar, 1971). Contact mineral assemblages suggest emplacement of the Winnsboro pluton under conditions of low-pressure metamorphism (Miyashiro, 1973) similar to, but perhaps slightly cooler than, the Liberty Hill pluton of similar age ( $299 \pm 8$  m.y., Fullagar, 1971). The Liberty Hill pluton has xenoliths with assemblages in the pyroxene hornfels facies (Speer, VPI&SU-5103-3, p. A30). Such high-temperature assemblages have not been found in the xenoliths of the Winnsboro pluton.

The Rion pluton, which occupies the core of the Winnsboro complex, appears to have been intruded as a cooler, wetter magma than the coarse-grained Winnsboro pluton. This is reflected in its mineralogy. It is a biotite granite, while the Winnsboro pluton is a drier biotite-hornblende granite. The lower temperature of intrusion is also reflected in xenolith mineralogy. One sample from the very southern edge of the Rion pluton has the assemblage:

biotite-cordierite-muscovite-microcline-fibrolite-quartz

(F7-47, Fig. A2).

However, the fibrolite occurs as small relict(?) patches in large muscovite grains which appear to be replacing it. It is quite possibly an assemblage formed in the contact aureole of the Winnsboro pluton and partially retrograded by the Rion pluton. The few, tiny xenoliths found within the interior of the Rion pluton have the assemblage:

muscovite-biotite-epidote-plagioclase-quartz

and appear to be even somewhat lower in grade.

Delimitation of a contact aureole for the Rion pluton would be extremely difficult, since it would require differentiating the effects of three metamorphic events--the regional metamorphism, the contact metamorphism of the Winnsboro pluton, and the contact metamorphism of the Rion pluton.

#### Summary

In the area of the Winnsboro complex, a regional medium-pressure metamorphic event which reached the amphibolite facies was followed by deformation and uplift with decrease in regional temperature and pressure. The Winnsboro complex was intruded with a resultant low-pressure contact metamorphism which reached hornblende hornfels grade in the xenoliths of the relatively dry Winnsboro biotite-hornblende granite and somewhat lower grade in xenoliths of the later, wetter Rion biotite granite.



## The Petersburg Batholith

Andy R. Bobyarchick

### Regional Setting

The Petersburg batholith comprises three roughly elliptical plutons in the eastern Virginia Piedmont which underlie approximately 7100 km<sup>2</sup> (2700 mi<sup>2</sup>) of area west of the fall line in the Coastal Plain (Calver, 1963). These plutons (of the Petersburg batholith) are defined on the basis of their geographic location: 1) the eastern pluton, which crops out from Ashland north of the James River to Dinwiddie County southwest of Petersburg; 2) the southern pluton, which crops out in Brunswick and Greensville counties south of the Nottoway River to the North Carolina state line; and 3) the western pluton, exposed in a north-south trending elongate body extending from Hebron to the North Carolina state line (Fig. A6). Much of the eastern margin of the batholith is exposed only in the floors of dissected stream valleys in the Coastal Plain; this, in addition to extensive and locally deep weathering of the batholith surface, restricts the number of fresh outcrops available for sampling. Medium to coarse grained, weakly or non-foliated massive granite (Pgm) is the dominant lithology in the Petersburg batholith. Coarse grained, moderately foliated, locally lineated microcline granite porphyry (Pgp) and medium grained, moderately to strongly foliated gray granite or granodiorite (Pgf) complete the three primary phases of granitic rocks present. Minor exposures of a coarse grained microcline-quartz protoclastic border zone (Pgpr) occur around the northern terminus of the southernmost pluton (Fig. A7). This study has concentrated on the

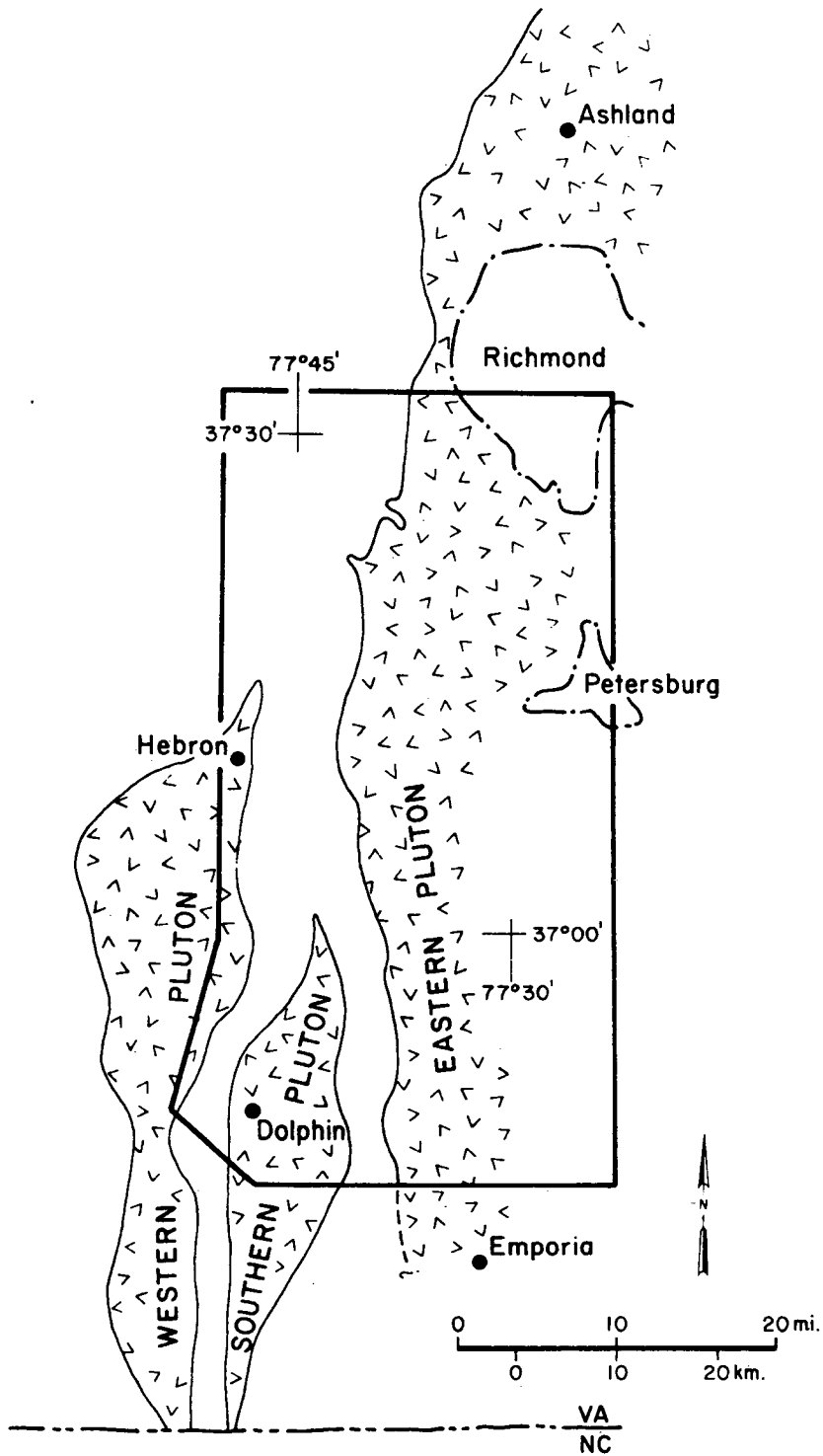
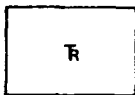


Figure A6. Index map showing location of the three named plutons of the Petersburg batholith and study area.

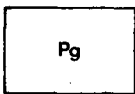
Explanation



Cretaceous to Tertiary Coastal Plain sediments.



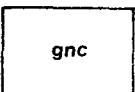
Triassic sedimentary rocks in the Richmond Basin.



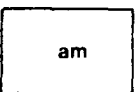
Petersburg batholith. Pgu--undifferentiated granite; Pgm--medium to coarse grained, weakly or non-foliated massive granite; Pgf--moderately to strongly foliated, medium grained gray granite; Pgp--coarse grained, moderately foliated, strongly lineated microcline granite porphyry; Pgpr--coarse grained protoclastic border.



Metamorphosed sedimentary and volcanic rocks. Includes: red and green laminated slate; quartz-muscovite phyllite; biotite-actinolite-epidote-chlorite-quartz gneiss; epidote-chlorite-plagioclase phyllite; muscovite-quartz schist; muscovite-quartz-feldspar gneiss; rhyodacite; greenstone and amphibolite.



Gneiss complex. Dominantly medium grained, muscovitic lineated granite gneiss with biotite schist and felsic gneiss selvages. A marginal layered sequence of locally garnetiferous prophyroblastic biotite schist, biotite gneiss and granite gneiss.



Coarse grained pyroxene-hornblende amphibolite.

Structure Symbols

- Geologic contact; dotted where covered.
- - - - - Gradational phase boundary in Petersburg batholith. Dotted where covered; queried where doubtful.
- - - - - Fault. Dashed where approximate; dotted where covered.
- AB77-53 Chemistry-heat production sample location.

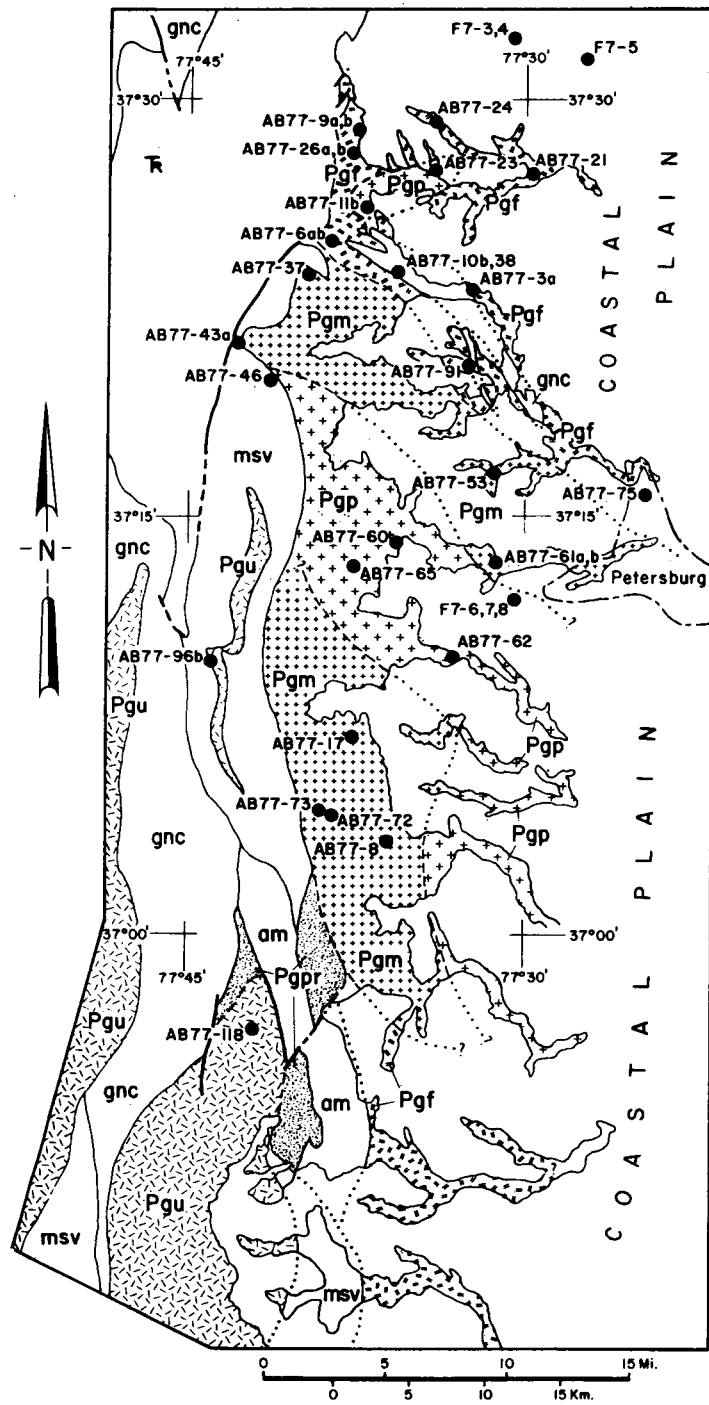


Figure A7. Geologic map of the eastern pluton of the Petersburg batholith.

eastern pluton, the largest in the Petersburg batholith (approximately 5350 km<sup>2</sup> (2033 mi<sup>2</sup>)).

Country rocks enclosing the three Petersburg plutons are grouped into two lithologic units, partially distinguished on the basis of metamorphic grade. High grade (lower to middle amphibolite facies) rocks bordering the western and southern plutons are dominantly medium grained granitic gneiss with minor biotite gneiss, biotite schist and amphibole gneiss (gnc, Fig. A7). Low grade rocks (lower greenschist to epidote-amphibolite) facies composed primarily of metamorphosed sedimentary and volcanic protoliths bound the eastern pluton and eastern margin of the southern pluton (msv, Fig. A7); muscovite schist and quartzite (msv) occur east of the western pluton in the southwest corner of the study area. A coarse grained metamorphosed diorite (am) containing hornblende and pyroxene crops out between the eastern and southern plutons. The Petersburg batholith intrudes all the rocks described.

Terrestrial clastic sedimentary rocks and coal of Upper Triassic age (Roberts, 1928, p. 137-139) occur in fault or nonconformable contact with country rocks or the Petersburg batholith. These rocks, which form the Richmond Basin, are generally quartz arkose, subarkose and hematitic mudstone with lesser amounts of coal and fanglomerate as marginal facies. The feather edge of the Coastal Plain overlap in the study area is characterized by a thin veneer of generally unconsolidated hematitic clay and arenite, and locally in upland areas by quartz cobble alluvial deposits. Quaternary alluvial sediments occur extensively in lowland creeks and along major rivers; these have been omitted from Figure A7.

### Previous Work

Mention of granite in the James River channel was made by Johann David Schöpfung in 1787 (p. 76-77) who wrote that the rocks appeared as ". . . a hardened dough whose constituents, when it was still soft and fluid, were not properly kneaded together." This is probably the first recognition of flow foliation and xenoliths in the batholith.

Watson (1906) described three phases of granitic rocks from the Richmond and Petersburg areas: (1) light gray, medium to coarse grained granite with phenocrysts from 1 mm to 5 mm long (the Richmond-Petersburg light gray granite), (2) a finer grained dark blue granite of approximately the same composition (the Richmond-Fredericksburg dark blue gray granite), and (3) in the vicinity of Midlothian, a porphyritic granite with euhedral potassium feldspar phenocrysts as much as 5 cm (2 in) long. He believed the blue granite to be intrusive into the gray granite.

All granitic rocks south of Richmond to the North Carolina state line were shown as "Petersburg granite" on the 1928 Geologic Map of Virginia (Stose, 1928). Shortly thereafter, Jonas (1932, p. 243) referred to undeformed granite in the Virginia Piedmont as "Petersburg granite." Bloomer (1939) recognized three phases of Petersburg granite in the Richmond to Petersburg area but, unlike Watson (1906), regarded them as being contemporaneous, the blue granite representing an area of assimilation of gneissic country rocks. The three phases reported by Watson (1906) and Bloomer (1939) correspond to the porphyritic, massive and foliated phases described in this report, which are considered contemporaneous. Bloomer (1939, p. 141) recognized the batholithic proportions of Petersburg granite in Virginia. The great lateral extent and apparent consanguinity of the three plutons formerly

shown as Petersburg granite (Calver, 1963), as well as ambiguity in the definition of this granite, require that the nomenclature "Petersburg batholith" be used.

Recent work involving mapping and petrography of portions of the Petersburg batholith include Goodwin (1970), Weems (1974), and Bobyarchick (1976).

### Metamorphic Rocks

Metamorphic country rocks around the Petersburg batholith are grouped into two units. A complete description of the mineralogy and structure of these units is beyond the scope of this report, and only brief discussions are provided.

#### Gneiss complex (gnc)

Lineated, medium to coarse grained (0.5 mm to 0.8 mm) muscovite granite gneiss (generally less than 10% mafics) with numerous biotite schist and feldspathic gneiss segregations constitute the primary rock types in the gneiss complex. The granite gneiss possesses a weak compositional layering defined primarily by alternating mafic and felsic bands, which, where intersected by the strongly developed primary biotite schistosity, forms a lineated fabric. Much of this unit is poorly exposed, but part of the marginal zone of the gneiss complex, especially along the eastern border, may be characterized by an intercalated sequence of locally garnetiferous, porphyroblastic (plagioclase) biotite schist, biotite gneiss, and felsic gneiss and minor amphibole gneiss.

The dominant, lineated granite gneiss is thought to be of igneous origin because of a regionally homogeneous composition and probable granitic or

granodioritic pre-metamorphic composition. Layered gneisses in the gneiss complex may be higher grade equivalents of lithologies in the msv unit.

Biotite gneiss and hornblende-biotite gneiss (gnc) occur in an elongate septum of country rock surrounded by granite in the Petersburg batholith northwest of Petersburg (Fig. A7). These gneisses, generally migmatitic, were intruded locally by discordant felsic dikelets or pegmatites. The septum has been included on Figure A2 as part of the gneiss complex.

#### Metamorphosed sedimentary and volcanic rocks (msv)

Metamorphosed sedimentary and volcanic rocks in the msv unit occur primarily along the western margin of the eastern Petersburg granite; smaller belts of this unit lie adjacent to the other two plutons (Fig. A7). The appearance of these rocks is variable because of regional and thermal metamorphism. Low grade rocks are slates and quartzites; intermediate rocks generally appear as phyllites or quartzose gneisses with phyllitic laminations and greenstone, and higher grade rocks on the margins of the unit occur as mica schist and gneiss and amphibolite.

Volcaniclastic rocks. Rocks of probable volcaniclastic origin consist of: red and green laminated, fine grained slate with interlayered sandstone lenses; quartz-muscovite phyllite; quartzite; biotite-actinolite-epidote-chlorite-quartz gneiss and epidote-chlorite-plagioclase phyllite. Muscovite-quartz schist and muscovite-quartz-feldspar gneiss near the western Petersburg pluton are included in this group of rocks.

Although largely of undetermined origin because of the regional metamorphism, this group of rocks is thought to be dominantly volcaniclastic. No coarse pyroclastic rocks were observed but one sample of fine grained



epidote-chlorite-plagioclase phyllite appears tuffaceous; several highly weathered felsite exposures may represent more felsic tuff. Rocks such as quartzite, mica-quartz slate and phyllite probably represent reworked volcaniclastic sediments or epiclastic rocks present in the low grade belt.

Volcanic rocks. Hypabyssal and extrusive volcanic rocks are relatively minor in the study area and probably make up less than 15 percent of the total volume of rocks present. They occur along the western and eastern margins of the msv unit and are conformable structurally upward with volcaniclastic rocks.

Rhyodacite constitutes the felsic compositions present while greenstone or fine grained amphibolite, probably originally of basaltic composition, in minor amounts represent the more mafic compositions. Intermediate compositions seem to be restricted to pyroclastic units.

Volcanic rocks in the msv unit occur primarily along the margins of the central belt of rocks west of Petersburg and are perhaps also represented in the layered sequence(s) of the gneiss complex.

#### The Petersburg Batholith

Three mapable phases are recognized in the Petersburg batholith, but only the eastern pluton has been subdivided on Fig. A7. Generally, all three phases are modally granites so that phase designations are based on grain size and texture. With the exception of coarse grained microcline granite porphyry, which contains euhedral microcline phenocrysts, all rocks are hypidiomorphic granular to allotriomorphic granular and massive. However, some foliated phases show incipient compositional layering and shape oriented fabrics. The primary mineralogy comprises quartz, plagioclase,

microcline and less than (about) five percent green-brown biotite with minor amounts of muscovite, allanite and titanite. All phases appear broadly gradational at contacts and are therefore probably approximately contemporaneous.

Massive phase (Pgm). The dominant rock in the Petersburg batholith is a medium to coarse grained, weakly- or non-foliated, massive pink biotite granite with grain sizes of 5 mm to 1 cm. Most microcline is microperthitic. Myrmekite was locally developed. This phase contains schlieren a few cm long formed by biotite aggregates, especially in marginal zones close to country rocks.

Porphyritic phase (Pgp). Coarse to very coarse grained, locally strongly lineated, moderately foliated porphyritic microcline granite crops out in a northwest to southeast trending belt along the medial part of the eastern Petersburg pluton. This phase contains euhedral microcline phenocrysts as much as 3 cm long and as much as 8 percent biotite. Most exposures of granite porphyry have a strongly lineated fabric defined by colinear orientations of the microcline phenocrysts and weak shape orientation of quartz.

Foliated phase (Pgf). Fine to medium grained, moderately to strongly foliated biotite (5 to 15 percent) granite is the most poorly exposed phase of the Petersburg batholith; some varieties may be granodiorite. Weak compositional layering, defined mainly by segregation of mafic and felsic minerals, developed locally, is best expressed at the contact with the gneiss complex septum in the pluton (Fig. A7). Xenoliths are more abundant in the foliated phase than in the massive or porphyritic phases, and rare exposures of the country rock/foliated phase contact indicate that assimilation of micaceous country rock may be responsible for a higher percentage of biotite in the

foliated phase. Xenoliths of biotite schist and clots of biotite in the granite also characterize these contact zones.

Protoclastic border zones (Pgpr). Three discrete zones of protoclasis occur at the northern end of the southern Petersburg pluton and southeastern end of the eastern pluton (Fig. A7) and were coeval with intrusion of the batholith because they are gradational into less sheared granite. Strongly elongate quartz and microcline and minor muscovite constitute this phase of granite, and this fabric is attributed to localized high strain rates at the time of intrusion.

#### Regional Metamorphism

All rocks in the gneiss complex and metamorphosed sedimentary and volcanic rock unit have been subjected to metamorphism ranging from middle greenschist to lower amphibolite facies. Brown or orange-brown biotite, muscovite, brown-green hornblende, garnet, quartz, microcline and sodic to intermediate plagioclase occur in rocks of the gnc unit. Calcic pyroxene and kyanite have been reported from similar schists and gneisses north of the James River (Bobyarchick, 1976). These minerals are characteristic of the lower amphibolite facies (Miyashiro, 1973, p. 305-306). In the msv unit epidote, chlorite, biotite, actinolite, calcite, quartz, muscovite and albite of metamorphic origin are present. In some volcanic rocks, intermediate plagioclase has epidotized cores and locally may have albitic rims. These assemblages suggest middle to upper greenschist facies (Miyashiro, 1973, p. 304).

## Structure

A detailed discussion concerning the structural history in the eastern Virginia Piedmont is given by Bobyarchick (1976) and Bobyarchick and Glover (1977, submitted for publication). The following section, therefore, is a brief review of this tectogenesis intended to provide a framework for the structural setting of the emplacement and later modification of the Petersburg batholith. Table A2 lists the various structural elements and correlates them to their respective deformational events.

### Ductile deformations

Two periods of ductile deformation ( $D_1, D_2$ ) were approximately coeval with regional prograde metamorphism in rocks which reached amphibolite facies. The thermal peak of metamorphism probably occurred at about 340 m.y. ago (discussion in Bobyarchick, 1976, p. 84).

$D_1$ , the principal deformational event, resulted in a pervasive schistosity in the gnc unit and phyllitic lamination or slaty cleavage in the msv unit ( $S_1$ ). In rare outcrops where original sedimentary or pyroclastic layering ( $S_b$ ) was preserved,  $S_1$  generally transects  $S_b$  at about 30 degrees. Most mesoscopic compositional layering in gneissic rocks ( $S_0$ ) is probably of metamorphic origin.

$S_2$ , a non-pervasive cleavage formed during  $D_2$ , is of slightly different character in the msv unit than in the gnc unit. Microstructures indicate that in amphibolite facies rocks,  $D_2$  was accompanied by a subtle recrystallization and perhaps reorientation of biotite folia ( $S_2$ ) generally associated with  $F_2$  folding. Well-equilibrated grain boundaries and lack of strain suggest the thermal episode maintained a fairly consistent temperature

TABLE A2. STRUCTURAL ELEMENTS.\*

Element			Def. Event
<u>Planar Elements</u>			
Primary layering	Bedding ( $S_b$ ), compositional layering	( $S_0$ )	-
Pervasive tectonic surfaces	Schistosity axial planar to $F_1$ folds	( $S_1$ )	$D_1$
	Cleavage axial planar to $F_2$ folds	(rare) ( $S_2$ )	$D_2$
Igneous foliation	Planar orientation of mica folia and shape orientation of quartz and microcline	( $S_g$ )	$D_2$
<u>Linear Elements</u>			
Intersections	$S_1, S_2$ line or groove on $S_1$ surfaces	( $L_{1x2}$ )	$D_2$
	$S_0, S_1$ line or groove on $S_0$ surfaces	( $L_{0x1}$ )	$D_1$
Fold axes	Axes of folds, crenulations or systematic undulations	( $F_1$ )	$D_1$
		( $F_2$ )	$D_2$
Elongate minerals, mineral alignment	Elongated minerals	feldspar ( $L_{ef}$ )	$D_2$
		hornblende ( $L_h$ )	$D_2$
	Aligned minerals	biotite ( $L_b$ )	$D_2$

\*Modified from Bobyarchick and Glover (1977, submitted for publication).

throughout  $D_2$ . However,  $S_2$  occurs either as a simple rock cleavage (in slates and some phyllites) or gentle crenulation of  $S_1$  (in pyroclastic and upper greenschist rocks) with incipient chlorite recrystallization along the crenulations in the msv unit. The implication here is that the rheological nature of  $D_2$  is more ductile with increasing metamorphic grade.

Paleozoic post-metamorphic deformation was most intense north of the study area in the Hylas zone (Bobyarchick and others, 1976; Bobyarchick, 1976). This period of shearing is represented south of the James River by minor discrete chloritized shears generally localized along the margins of Petersburg plutons. It is possible that folding of  $S_1$  in the msv unit could have occurred at this time.

Brittle fracturing and faulting of rocks in the study area occurred about 220 m.y. ago (Bobyarchick, 1976, p. 78) during the Triassic and resulted in the formation of a structural depositional basin, the Richmond Basin. Intense fracturing and jointing of the crystalline basement was accompanied by zeolite mineralization.

#### Emplacement of the Petersburg Batholith

Foliated phases of granite in the study area have a planar orientation of biotite folia and tabular microcline phenocrysts and shape orientation of quartz which form a foliation herein designated as  $S_g$ . Quartz in the foliated granites was ubiquitously partially recrystallized and very diffuse, irregular subgrain boundaries were produced in phenocrysts.

Mapping in the contact zone revealed that intrusion of the granite obviously post-dated  $D_1$ :  $S_1$  was plastically deformed and the rocks were partially migmatized. In the gneiss complex septum, which is wholly enclosed

by granite,  $S_1$  and  $S_0$  were locally deformed into rather open folds where a reorientation and, perhaps, recrystallization of biotite folia produced an axial plane cleavage. On the edge of the pluton, apophyses of granite locally occupy core zones in folded country rocks which appear to have formed at the time of intrusion. Here, and elsewhere in the contact zone, late non-foliated felsic dikes run undeformed through granite and country rocks.

Recrystallization in the contact zone varies according to the pre-emplacment lithologies. Where amphibolite facies rocks such as biotite gneiss or amphibolite were intruded, the principal effect was overall recrystallization. In these zones, straight grain boundaries predominate and little strain is evident. However, some rocks in the msv unit, especially those which were not totally recrystallized by contact metamorphism, show evidence of static recrystallization across  $S_1$ . In these rocks, euhedral actinolite grew directly across mica schistosity and some biotite formed poikilitic folia with highly irregular grain boundaries. Very fine mimetic biotite blebs parallel to  $S_1$  are also present. Near Winterpock, Virginia, at the northern end of the msv unit, a metabasite was apparently altered by intrusion of granite. It now occurs as a banded gneiss with alternating layers of pyroxene (diopside?)-calcite-tremolite(?)-epidote-plagioclase and hornblende-plagioclase. Along the central western margin of the eastern Petersburg pluton, a fine grained, pyritiferous, poorly foliated, highly deformed massive chlorite-epidote-quartz rock characterizes the contact zone.

The importance of these microstructural relationships and localized recrystallization near batholith contacts is that they are the result of modification by intrusion of the Petersburg batholith and did not occur

away from the contact zones. Therefore, these criteria can be used to describe the emplacement history of the batholith.

### Discussion

Wright, Sinha and Glover (1975) published a consolidation age for Petersburg granite, based on zircon studies, of  $330 \pm 8$  m.y. If the peak of regional metamorphism did occur about 340 m.y. ago, as has been assumed, then the Petersburg batholith would be a late metamorphic intrusion. The igneous foliation,  $S_g$ , would not be only the result of metamorphic recrystallization but may also be due to crystallization of a semi-plastic magma in a regional stress field. Since the granite is known to deform and partially recrystallize  $S_1$ , this stress field must have been that operative during the  $D_2$  deformational event. Thus,  $S_g$  is chronologically equivalent to  $S_2$ , although their mechanisms of formation differ.

Plots of poles to  $S_1$  and observations from field mapping indicate that rocks in the msv unit were deformed into a north to northwest trending synformal structure plunging gently to the northwest. Because the Petersburg batholith appears to be a  $D_2$  intrusion, this synform was most likely an  $F_2$  fold formed by deformation in the country rocks between the three plutons of the Petersburg batholith. Small scale folding around stocks of granite on margins of the batholith were contemporaneous with generation of the regional  $F_2$  synform. Post-metamorphic folding of the synform and granite is also indicated by similar disruption of plots of poles to  $S_1$  and  $S_g$ . This deformation may have occurred in response to shearing with northwestward vergence along the Hylas zone to the north (Bobyarchick, 1976). Brittle fracturing in Triassic time overprinted sections of the eastern and southern plutons.



## References

- Bloomer, R. O., 1939, Notes on the Petersburg Granite: Virginia Geol. Survey Bull., vol. 51-F, p. 137-145.
- Bobyarchick, A. R., 1976, Tectogenesis of the Hylas zone and eastern Piedmont near Richmond, Virginia (M.S. thesis): Virginia Polytechnic Institute and State University, Blacksburg, 168 p.
- Bobyarchick, A. R., Glover, Lynn, III, Weems, R. E., and Goodwin, B. K., 1976, The Hylas "volcanic" rocks northwest of Richmond are cataclastically retrograded gneisses (abs.): Geol. Soc. America Abs. with Programs, vol. 8, no. 2, p. 138.
- Bobyarchick, A. R., and Glover, Lynn, III, 1977, Deformation and metamorphism of the Hylas zone and eastern Piedmont in Virginia: submitted for publication.
- Butler, J. R., 1966, Geology and mineral resources of York County, South Carolina: S. C. State Devel. Board, Div. of Geol., Bull. 33, 65 p.
- Calver, J. L., 1963, Geologic map of Virginia: Virginia Division of Mineral Resources.
- Espenshade, G. H., and Potter, D. B., 1960, Kyanite, sillimanite, and andalusite deposits of the southeastern states: U. S. Geol. Survey Prof. Paper 336, 121 p.
- Fullagar, P. D., 1971, Age and origin of plutonic intrusions in the Piedmont of the southeastern Appalachians: Geol. Soc. America Bull. 82, p. 2845-2862.
- Goodwin, B. K., 1970, Geology of the Hylas and Midlothian quadrangles, Virginia: Virginia Division of Mineral Resources, Rep. of Inves. 23, 51 p.
- Jonas, A. I., 1932, Structure of the metamorphic belt of the southern Appalachians: Am. Jour. Sci., 5th ser., vol. 24, p. 228-243.
- Miyashiro, A., 1973, Metamorphism and Metamorphic Belts: New York, John Wiley & Sons, Inc., 492 p.
- Overstreet, W. C., and Bell, H., III, 1965, The crystalline rocks of South Carolina, U. S. Geol. Survey Bull. 1183, 126 p.
- Overstreet, W. C., Overstreet, E. F., and Bell, H., III, 1960, Pseudomorphs of kyanite near Winnsboro, Fairfield County, South Carolina: Geologic Notes, Div. of Geol., S. C. State Devel. Board 4, p. 35-49.

- Richardson, S. W., Gilbert, M. C., and Bell, P. M., 1969, Experimental determination of kyanite-sillimanite equilibria: the aluminum silicate triple point: *Am. Jour. Sci.* 267, p. 259-272.
- Roberts, J. K., 1928, Geology of the Virginia Triassic: *Virginia Geol. Survey Bull.* 29, 205 p.
- Schöpf, J. D., 1787, Beiträge zur Mineralogischen Kenntniss des Ostlichen Theils von Nord-Amerika und seiner Geburge (Contributions to the mineralogical knowledge of the eastern part of North America and its mountains), in Spieker, E. M., translator, 1972, Contributions to the History of Geology, vol. 8: New York, Hafner Publishing Company, translation, 171 p.
- Secor, D. T., and Wagener, H. D., 1968, Stratigraphy, structure, and petrology of the Piedmont in central South Carolina: *S. C. State Devel. Board, Div. of Geol., Geologic Notes* 12, p. 67-84.
- Stose, G. W., editor, 1928, Geologic map of Virginia: *Virginia Geological Survey*.
- Wagener, H. D., 1970, Geology of the southern two-thirds of the Winnsboro 15-minute quadrangle, South Carolina: *S. C. State Devel. Board, Div. of Geol., MS-17*, 34 p.
- Wagener, H. D., 1973, Petrology of the adamellites, granites, and related metamorphic rocks of the Winnsboro quadrangle, South Carolina: *The Citadel, Monograph Series* X, 75 p.
- Watson, T. L., 1906, Lithological characters of the Virginia granites: *Geol. Soc. America Bull.* 17, p. 523-540.
- Wright, J. E., Sinha, A. K., and Glover, Lynn, III, 1975, Age of zircons from the Petersburg Granite, Virginia; with comments on belts of plutons in the Piedmont: *Am. Jour. Sci.*, v. 275, p. 848-856.

B. GEOCHEMISTRY

A. K. Sinha, Principal Investigator

B. A. Merz, Research Associate

## Win 1 Core Samples

Seventeen samples from the Win 1 bore hole were analyzed by x-ray fluorescence. The bore hole, nearly 1900 ft. deep, is the deepest to date and is located near the eastern margin of the Winnsboro-Rion pluton. All except one of the samples were 6-ft. lengths of core, the exception being a sample from depth interval 356 to 357.5 ft. which was a short section of fine-grained rock in an otherwise medium-grained core. The samples from 1390-1396 ft. and 1490-1496 ft. were fractured and considerably altered while the other samples appeared fresh.

The chemical data for the surface samples from the Winnsboro complex were given in Report No. VPI&SU-5103-2. Figure B-1 and Table B-1 give data from the drill core, and it can be seen that the major element concentrations compare closely with those from the Rion surface samples. The core samples are slightly higher in  $Al_2O_3$  than the surface samples but are still within the range of analytical uncertainty.

Figure B-1 shows that there is no regular change in either bulk composition or U and Th contents with depth. The U and Th abundances are those obtained by  $\gamma$ -ray spectrometry. The variations in  $SiO_2$ , FeO and  $K_2O$  seen on the figure might be related to zones of alteration as defined petrographically (see petrography section of this report). The two most obviously altered samples, from 1390 ft. and 1490 ft., are amongst the lowest in U and Th contents. It is believed that the altered zones have been oxidized, so loss of U from such zones in the soluble oxidized form is likely.

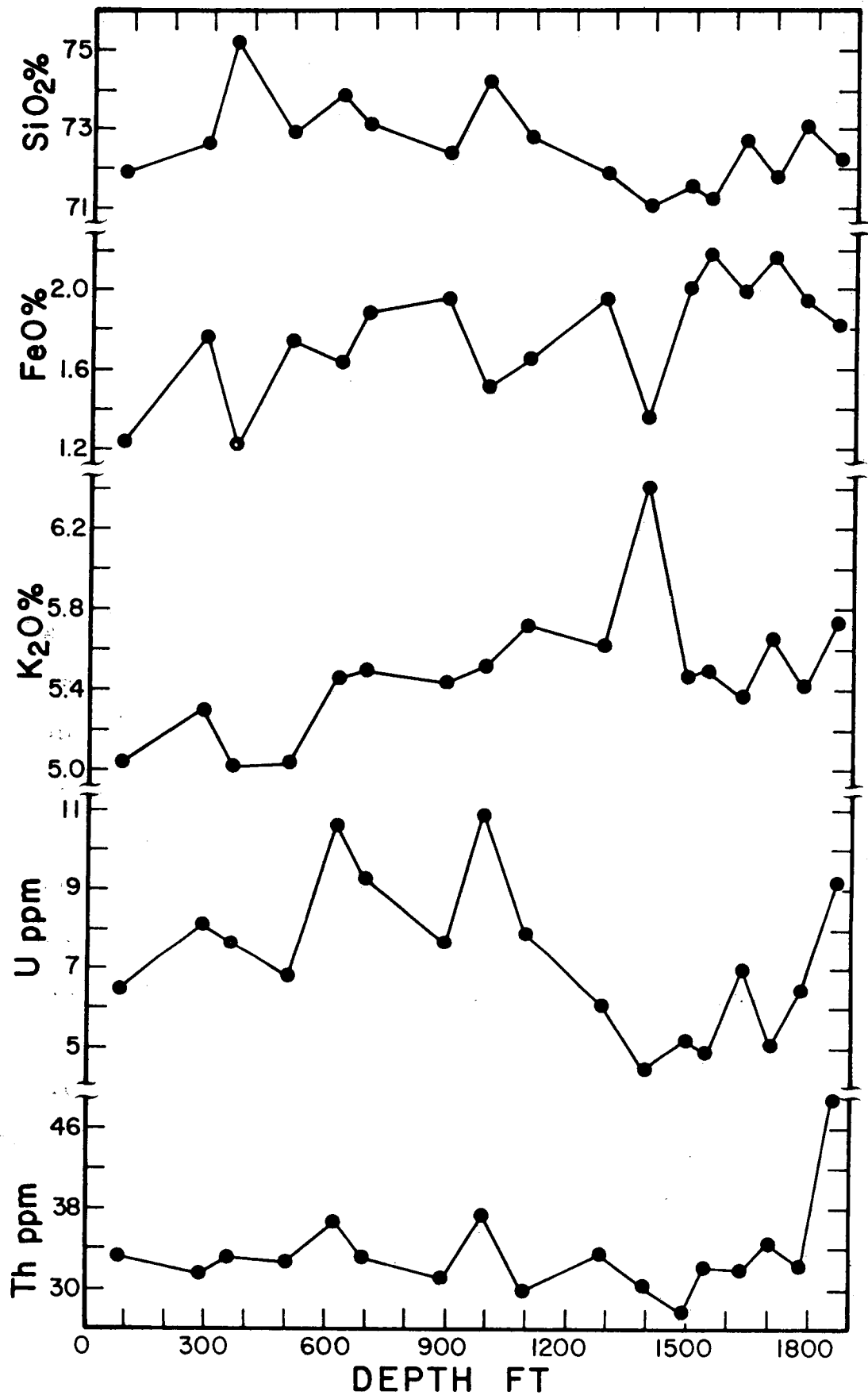


Figure B-1. Plot of SiO<sub>2</sub>, FeO, K<sub>2</sub>O, U, and Th with depth for bore hole Win 1.

Table B-1. Chemical compositions of Win 1 samples.

Depth, ft.	80	290	356	500	620	690	890	987
SiO <sub>2</sub>	71.88	72.61	75.36	72.96	73.94	73.14	72.39	74.26
Al <sub>2</sub> O <sub>3</sub>	15.17	15.08	14.92	15.08	14.94	15.46	15.63	15.28
CaO	1.33	1.38	1.26	1.46	1.30	1.31	1.56	1.25
MgO	.45	.48	.23	.42	.41	.42	.59	.37
K <sub>2</sub> O	5.19	5.30	5.03	5.04	5.46	5.49	5.44	5.52
FeO	1.85	1.77	1.23	1.75	1.64	1.90	1.96	1.52
Na <sub>2</sub> O	3.61	3.52	3.69	3.61	3.42	3.55	3.56	3.59
MnO	.05	.05	.04	.05	.05	.05	.07	.05
TiO <sub>2</sub>	.27	.25	.12	.23	.21	.25	.26	.18
P <sub>2</sub> O <sub>5</sub>	.09	.11	.05	.09	.09	.09	.12	.07
TOTAL	99.90	100.55	101.91	100.68	101.45	101.66	101.58	102.01

Table B-1 (continued).

Depth, ft.	1092	1281	1390	1490	1540	1630	1701	1779	1865
SiO <sub>2</sub>	72.78	71.87	71.08	71.59	71.28	72.77	71.84	73.09	72.27
Al <sub>2</sub> O <sub>3</sub>	15.39	15.89	16.49	15.52	15.66	15.40	15.90	15.28	15.91
CaO	1.35	1.62	1.39	1.52	1.58	1.43	1.50	1.39	1.37
MgO	.50	.58	.33	.48	.58	.48	.53	.45	.45
K <sub>2</sub> O	5.73	5.63	6.42	5.47	5.52	5.37	5.66	5.42	5.74
FeO	1.67	1.97	1.38	2.05	2.22	2.00	2.19	1.94	1.84
Na <sub>2</sub> O	3.55	3.46	3.46	3.50	3.43	3.51	3.48	3.55	3.59
MnO	.05	.05	.07	.09	.07	.05	.05	.05	.05
TiO <sub>2</sub>	.22	.25	.16	.24	.27	.26	.31	.25	.25
P <sub>2</sub> O <sub>5</sub>	.11	.12	.08	.12	.11	.10	.12	.10	.10
TOTAL	101.32	101.44	100.85	100.57	100.69	101.37	101.57	101.56	101.58

Figures B-2 and B-3 show U and Th plotted versus  $\text{SiO}_2$ . There is a strong positive correlation between U and  $\text{SiO}_2$ , the exception being sample 3, the fine-grained sample from 356 ft. There is also a reasonably good correlation between Th and  $\text{SiO}_2$  if sample 3 is again excluded, although the deepest sample, number 17, has anomalously high Th. In our continuing effort to develop a correlation between bulk chemistry and U and Th, the index used by Tilling et al. (1970) was applied to our data. This index,  $\text{CaO}/(\text{K}_2\text{O} + \text{Na}_2\text{O})$ , is a measure of the alkalinity of a suite of rocks as well as a type of differentiation index within one suite.

As can be seen on Figure B-4, there is a strong negative correlation between this index and the U contents of the Win 1 samples. The correlation between the U contents and index values of the surface samples is less strong and this is an indication of the effects of surface processes on the distribution of U and Th in such samples. All the plutons considered here are calc-alkaline; more alkaline suites should show similar trends displaced towards higher U.

Preliminary lead isotopic data suggest that the plutons may be older than the ages given by the Rb-Sr method, approximately 380 m.y. as opposed to 300 m.y.



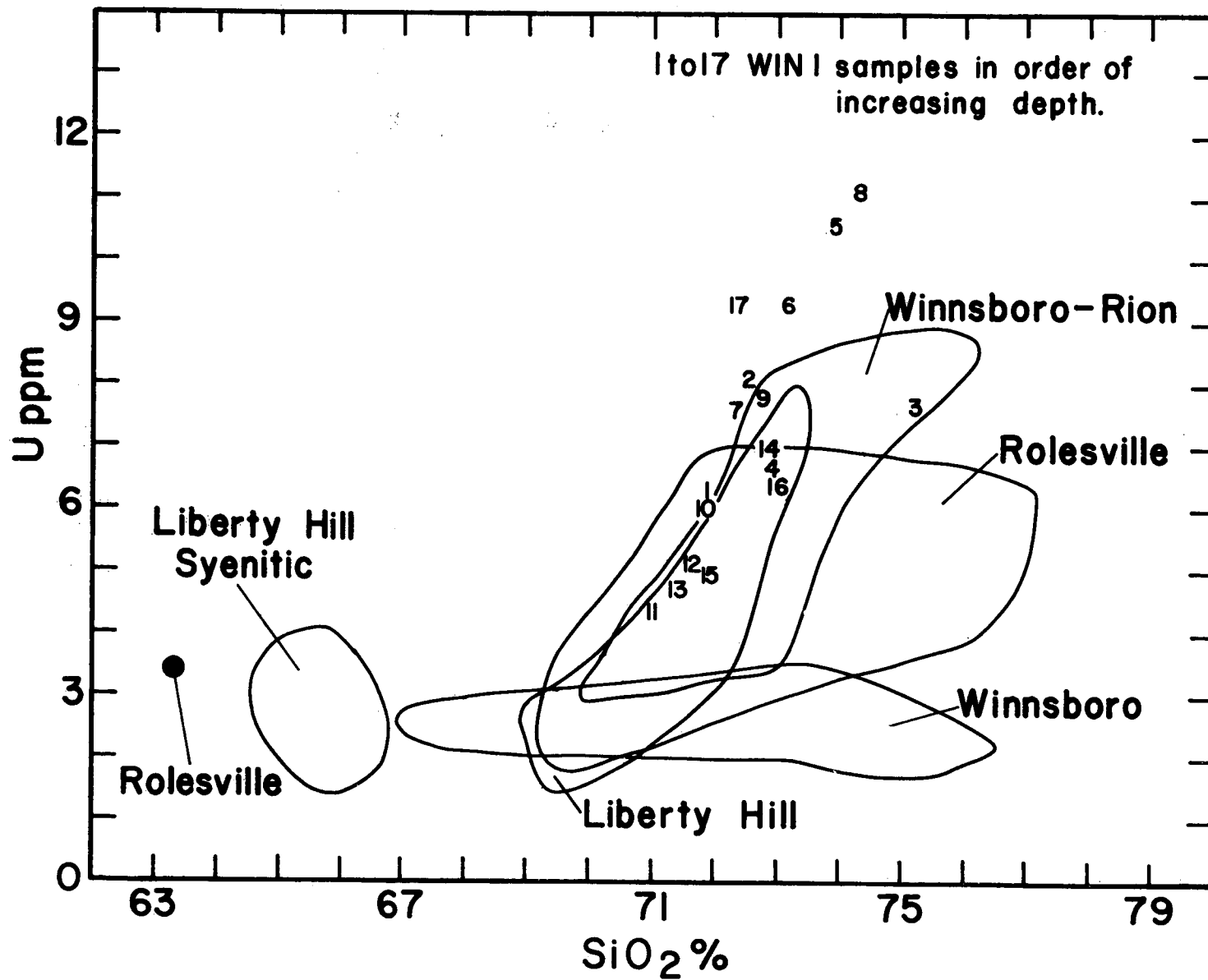


Figure B-2. U plotted vs. SiO<sub>2</sub> for Win 1 bore hole.

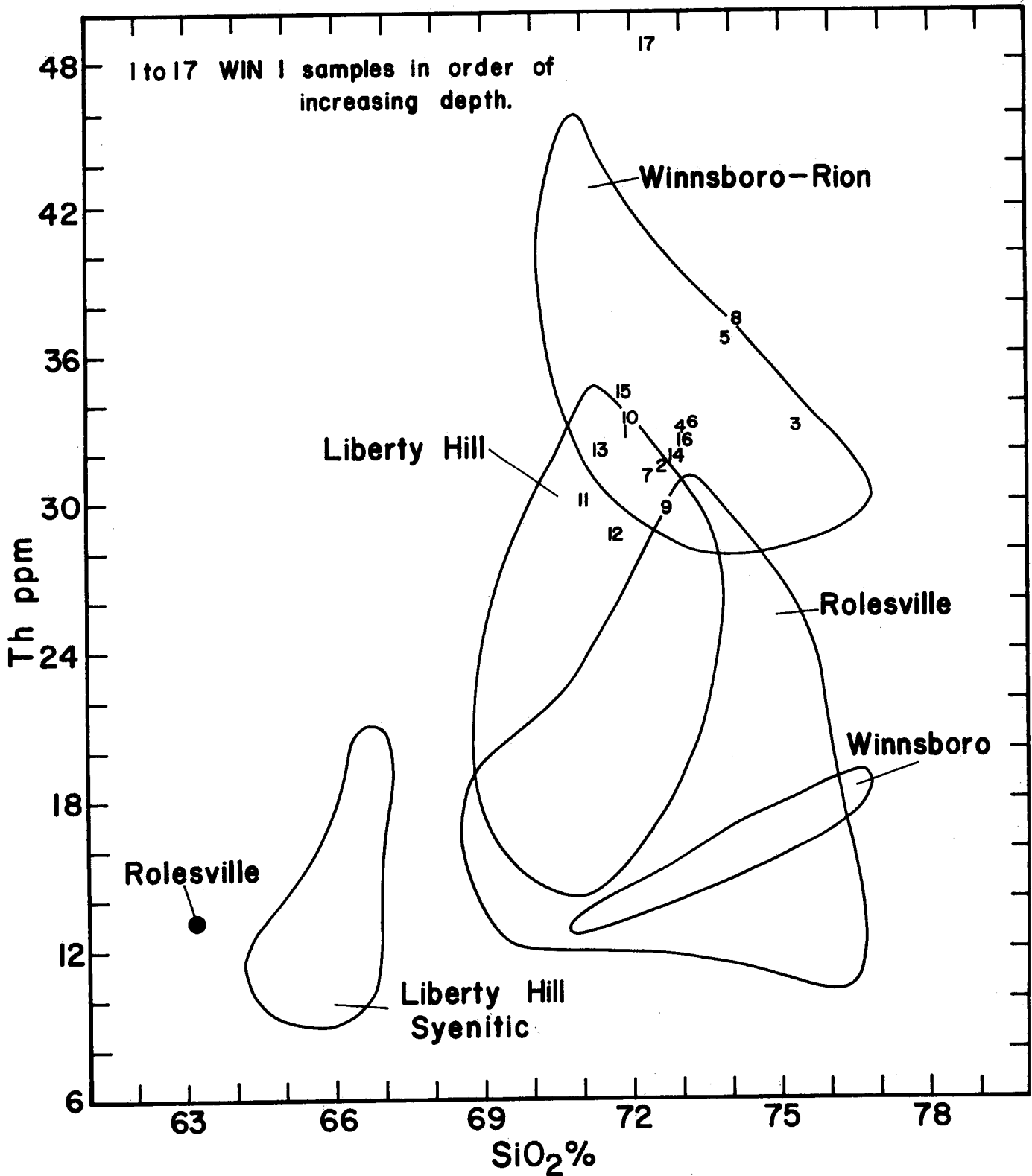


Figure B-3. Th plotted vs. SiO<sub>2</sub> for Win 1 bore hole.

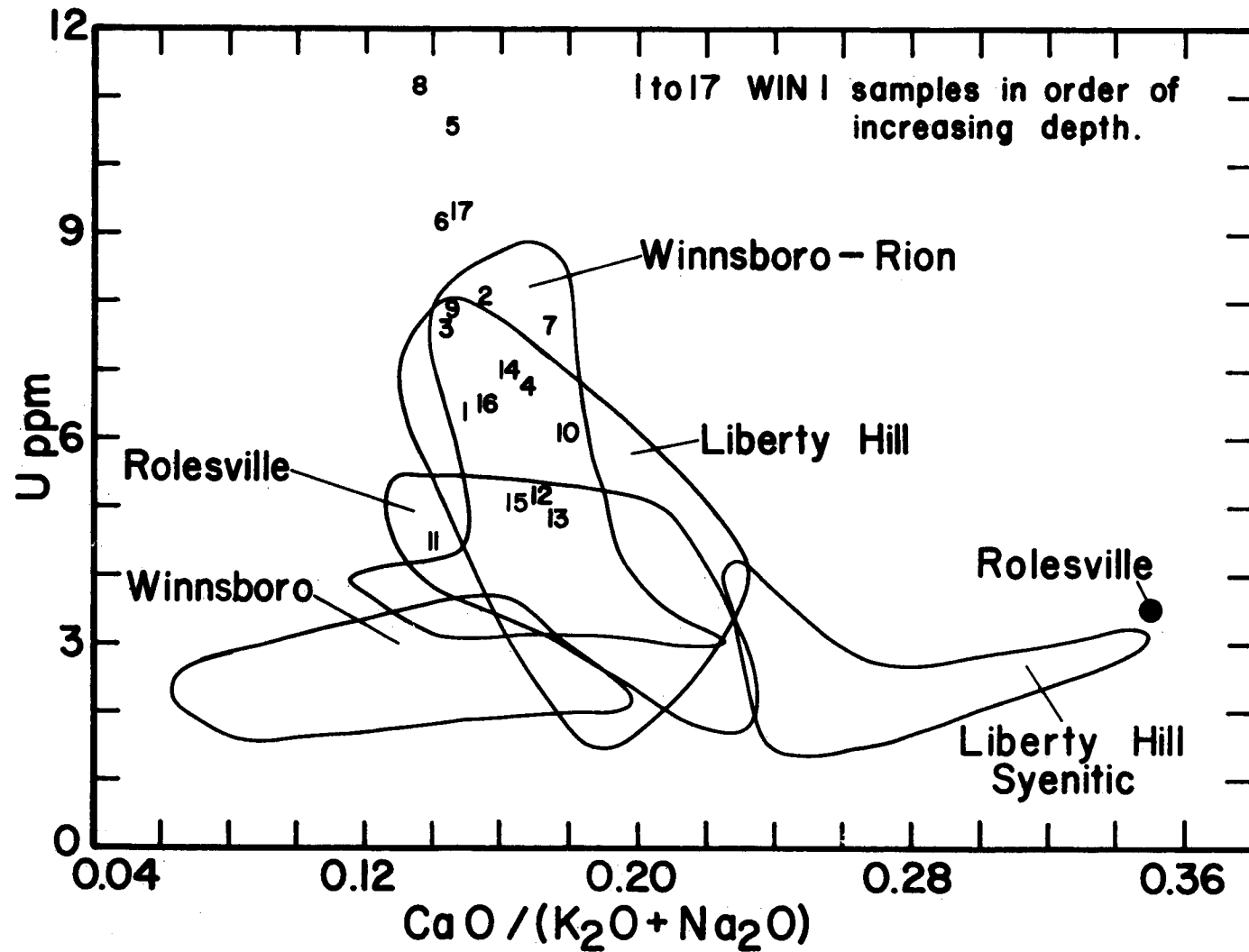


Figure B-4. Correlation between U and  $\text{CaO}/(\text{K}_2\text{O} + \text{Na}_2\text{O})$  for bore hole Win 1.

C. GEOPHYSICS

John K. Costain, Principal Investigator

Lawrence D. Perry, Research Associate

John A. Dunbar, Research Specialist

## Geothermal Gradients and Heat Flow

J. K. Costain, L. D. Perry, and J. A. Dunbar

Figure C-1 shows locations of holes drilled to date by VPI & SU in the southeastern United States. Temperature profiles and gradients at some of these locations are shown in Figure C-2.

Table C-1, which appears for the first time in this report, summarizes geothermal gradients, thermal conductivity, and heat flow determinations available to date for this contract. This table will appear in subsequent reports, and will be periodically updated as thermal conductivity values and heat flow determinations become available.

Geothermal gradients are determined by fitting a least-squares straight line for intervals in the hole over which the gradient is observed to be approximately constant. Subsequent reports may show slight changes in the geothermal gradient as holes reach thermal equilibrium and recover from the effects of drilling; changes in gradients are not expected to be more than a few percent (VPI&SU-5103-3, p. C-2).

Thermal conductivity determinations are made on a divided-bar apparatus (Costain and Wright, 1973). Rock discs are prepared from core from the same interval for which the geothermal gradient is reported. During measurement, the sample is maintained at a temperature of within 5°C of the in situ temperature. An axial stress of approximately 100 bars is applied to minimize thermal contact resistance. Conductivities are determined using discs 1.055" (2.680 cm) in diameter and 0.25" (0.635 cm) and 0.50" (1.270 cm) in thickness. Air is evacuated from all samples prior to flooding with distilled water.

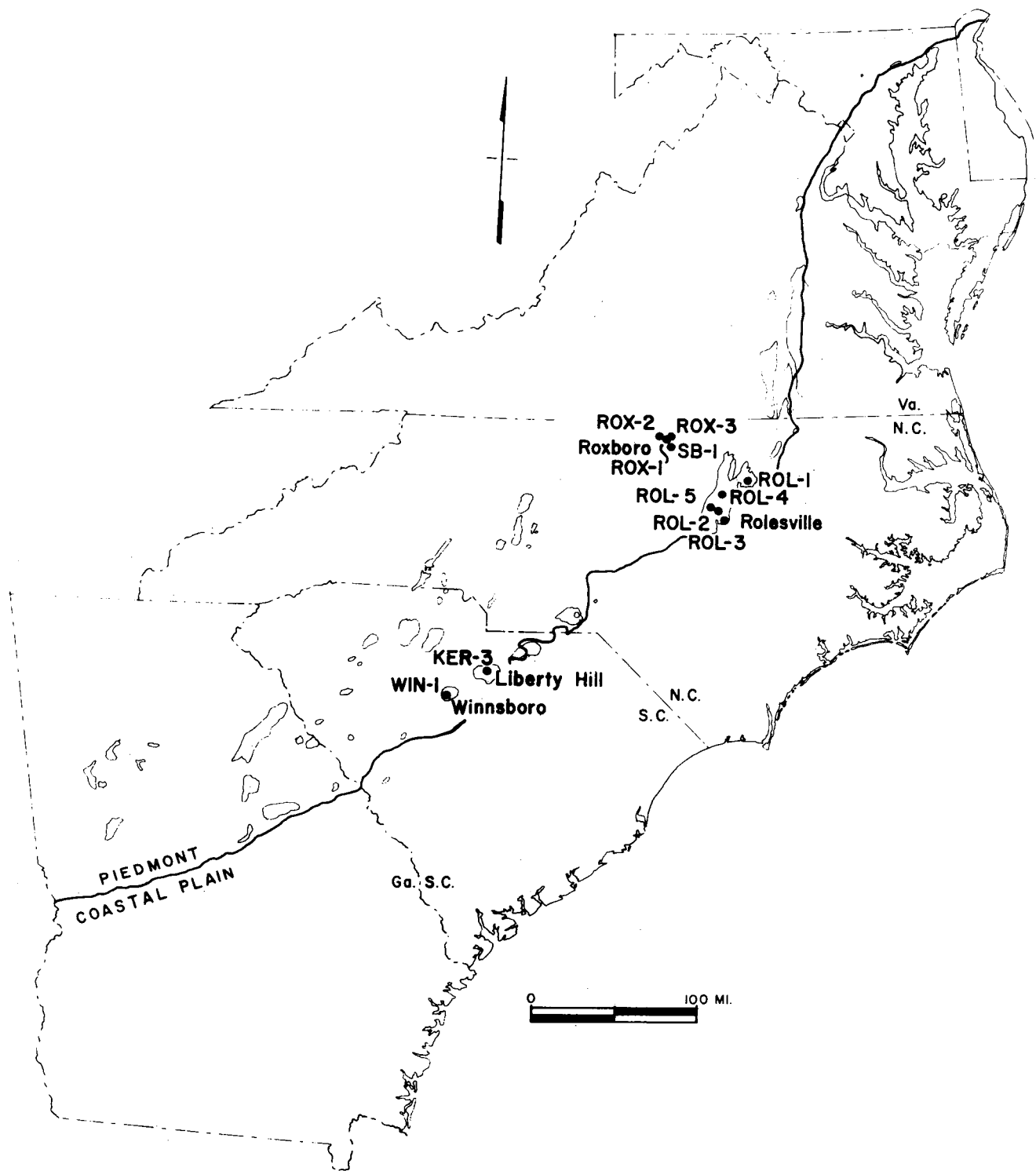


Figure C-1. Locations of holes drilled by VPI & SU in southeastern United States.

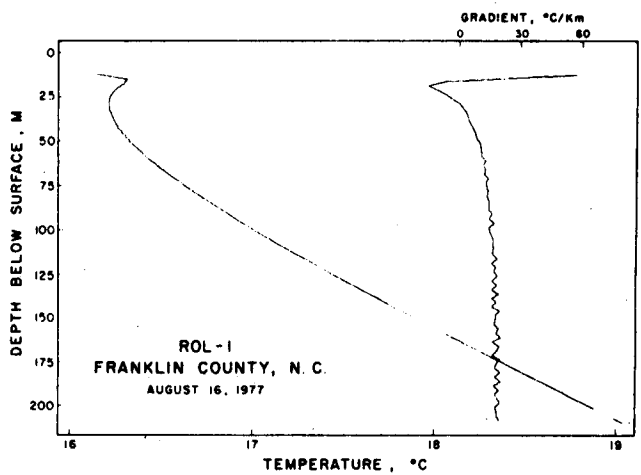
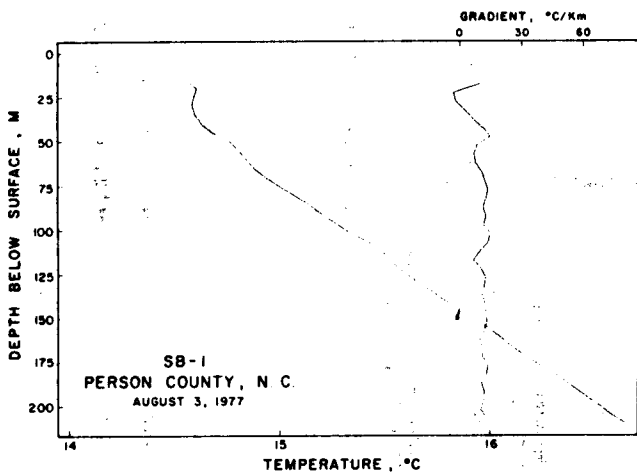
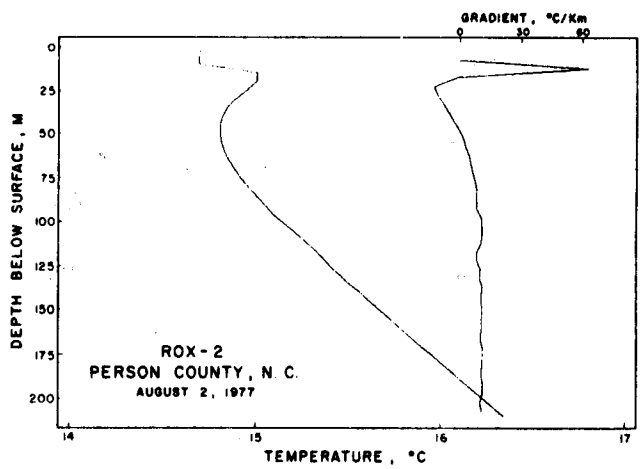
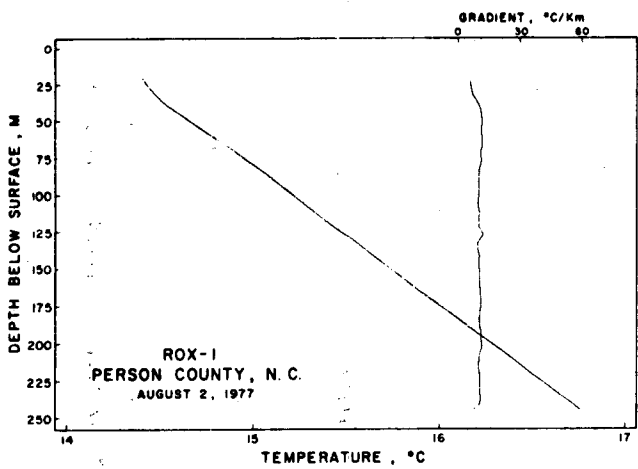
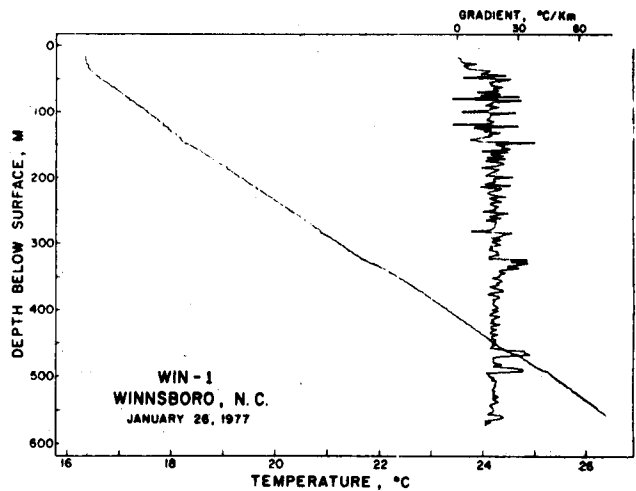
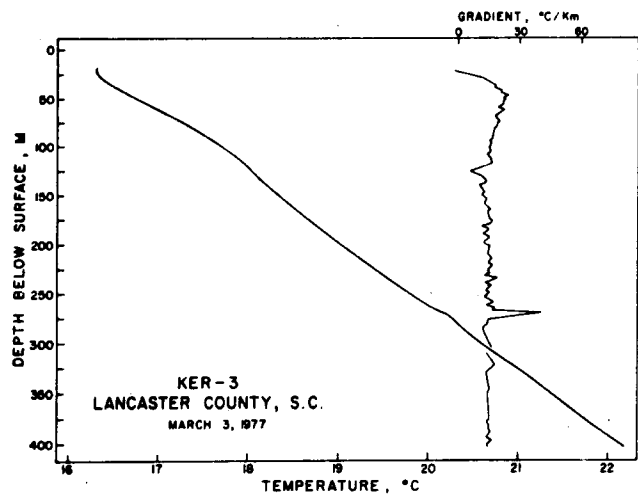


Figure C-2. Temperature profiles and gradients in holes drilled by VPI & SU.

Table C-1. Summary of heat flow data.

LOCATION	LATITUDE	LONGITUDE	DATE LOGGED	HOLE DEPTH (METERS)	DEPTH INTERVAL (METERS)	GRADIENT <sup>3</sup> ( °C/KM)	CONDUCTIVITY <sup>3</sup> (MCAL/CM-SEC- °C)	HEAT FLOW ( μ CAL/CM <sup>2</sup> -SEC)
<b>LIBERTY HILL - KERSHAW PLUTON, LANCASTER CO., S. C.</b>								
KER-3	34°32' 20"	80°44' 51"	11/18/76	277	316.8-404.3	14.91 ± 0.02 (36)	7.14 ± 0.57 (24) <sup>4</sup>	1.07 ± 0.09 <sup>1</sup>
					334.3-341.8	14.68 ± 0.07 (4)	6.94 ± 0.47 (3) <sup>4</sup>	1.02 ± 0.07 <sup>1</sup>
								1.02 ± 0.03 <sup>2</sup>
					344.3-356.8	15.06 ± 0.07 (6)	7.09 ± 0.54 (5) <sup>4</sup>	1.07 ± 0.09 <sup>1</sup>
								1.05 ± 0.02 <sup>2</sup>
					359.3-369.3	14.88 ± 0.07 (5)	7.33 ± 0.20 (4) <sup>4</sup>	1.09 ± 0.04 <sup>1</sup>
								1.09 ± 0.01 <sup>2</sup>
			371.8-384.3	14.85 ± 0.06 (6)	7.07 ± 0.28 (5) <sup>4</sup>	1.05 ± 0.05 <sup>1</sup>		
						1.05 ± 0.01 <sup>2</sup>		
				386.8-401.8	15.00 ± 0.13 (7)	6.94 ± 0.69 (6) <sup>4</sup>	1.04 ± 0.11 <sup>1</sup>	
							1.04 ± 0.01 <sup>2</sup>	
<b>WINNSBORO - RION PLUTON, FAIRFIELD CO., S. C.</b>								
WIN-1	34°18' 48"	81°08' 42"	7/5/77	570.3	24.24-571.74	18.18 ± 0.04 (220)	8.06 ± 0.24 (26)	1.47 ± 0.05 <sup>1</sup>
<b>ROXBORO METAGRANITE, PERSON CO., N.C.</b>								
ROX-1	36°23' 12"	78°58' 00"	5/19/77	240	146.8-249.3	10.83 ± 0.03 (42)	8.97 ± 0.41 (32)	0.97 ± 0.05 <sup>1</sup>
					146.8-184.3	11.03 ± 0.06 (16)	9.08 ± 0.11 (15)	1.00 ± 0.02 <sup>1</sup>
								1.00 ± 0.01 <sup>2</sup>
				219.3-231.8	10.94 ± 0.12 (16)	9.76 ± 0.59 (5)	0.96 ± 0.08 <sup>1</sup>	
							0.95 ± 0.01 <sup>2</sup>	
ROX-2	36°25' 31"	79°01' 53"	5/19/77	214	124.3-209.3	11.11 ± 0.02 (35)		
ROX-3	36°25' 39"	78°53' 42"	5/19/77	211.5	144.3-190.3	11.16 ± 0.88 (21)		



Table C-1 (continued).

LOCATION	LATITUDE	LONGITUDE	DATE LOGGED	HOLE DEPTH (METERS)	DEPTH INTERVAL (METERS)	GRADIENT <sup>3</sup> (°C/KM)	CONDUCTIVITY <sup>3</sup> (MCAL/CM-SEC-°C)	HEAT FLOW (μ CAL/CM <sup>2</sup> -SEC)
SLATE BELT PERSON CO., N.C.								
SB-1	36°19'40"	78°50'00"	6/5/77	211.5	81.7-181.7	11.70 ± 0.09 (28)		
ROLLESVILLE BATHOLITH, FRANKLIN CO., N.C.								
ROL-1	36°04'15"	78°07'43"	8/16/77	210.6	142.5-210.0	19.05 ± 0.11 (28)		
ROL-2	36°47'17"	78°25'04"		210.2				
ROL-3	35°57'05"	78°20'00"		121.9				
ROL-4	35°43'36"	78°19'45"		194.9				
ROL-5	35°51'17"	78°28'54"		ON SITE				

- 1 - INDICATES HEAT FLOW VALUE IS THE PRODUCT OF MEAN GRADIENT AND MEAN THERMAL CONDUCTIVITY  
2 - INDICATES HEAT FLOW VALUE IS FROM THE BULLARD APPROXIMATION  
3 - VALUE IN PARENTHESES IS THE NUMBER OF TEMPERATURE POINTS OR THE NUMBER OF THERMAL CONDUCTIVITY VALUES  
4 - THERMAL CONDUCTIVITY VALUES FROM 1.270 CM THICK SAMPLES ONLY

Thermal conductivity determinations are reported herein for Ker 3, Win 1, and Rox 1. Values are given in Tables C-2, C-3, and C-4. The mean conductivity of disks 1.270 cm in thickness is approximately 2% less than that determined for disks 0.635 cm in thickness. The standard deviation of the conductivity of the thinner disks is approximately 34% greater than that of the thicker disks, reflecting primarily the influence of crystal size and crystal orientation. Mean values of the thicker disks are used for heat flow values except for Rox 1.

Heat flow values are determined in two ways: (1) multiplication of the average thermal conductivity over the gradient for that interval, and (2) the Bullard approximation (Bullard, 1939). The results are the same within experimental error.

Table C-2.

Thermal conductivity values from Ker 3 core.  
(Samples are 2.680 cm. diameter.)

Sample Identification	Depth (meters)	Thermal Conductivity mcal/cm-sec-°C		
		Thickness	Thickness	%
		0.635 cm	1.270 cm	Difference
Ker3-1090	332.2	7.13	8.71	-8.1
Ker3-1100	335.3	7.06	6.42	+10.0
Ker3-1110	338.3	8.08	7.07	+14.3
Ker3-1120	341.4	7.82	7.33	+6.7
Ker3-1130	344.4	4.94	6.89	-28.3
Ker3-1140	347.5	8.24	7.35	+12.1
Ker3-1150	350.5	8.38	6.25	+34.1
Ker3-1160	353.6	6.94	7.38	-6.0
Ker3-1170	356.6	6.90	7.59	-9.1
Ker3-1180	359.6	8.19	7.56	+8.3
Ker3-1190	362.7	6.61	7.31	-9.6
Ker3-1200	365.8	7.71	7.07	+9.1
Ker3-1210	368.8	6.92	7.38	-6.2
Ker3-1220	371.9	8.61	7.27	+18.4
Ker3-1230	374.9	6.67	6.72	-0.7
Ker3-1240	378.0	7.71	7.04	+9.5
Ker3-1250	381.0	6.90	7.42	-7.0
Ker3-1260	384.1	6.72	6.89	-2.5
Ker3-1270	387.1	6.18	5.94	+4.0
Ker3-1281	390.5	7.31	7.05	+3.7
Ker3-1290	393.2	8.18	7.80	+4.9
Ker3-1300	396.2	6.02	6.30	-4.4
Ker3-1310	399.3	7.51	7.22	+4.0
Ker3-1320	402.3	7.90	7.35	+7.5
Mean		7.28	7.14	
Standard deviation		0.87	0.57	

Table C-3.

THERMAL CONDUCTIVITY VALUES FROM ROX-1 CORE  
(SAMPLES ARE 2.680 CM IN DIAMETER)

SAMPLE IDENTIFICATION	DEPTH (METERS)	THERMAL CONDUCTIVITY MCAL/CM-SEC-°C
RX1-486	148.1	8.828
RX1-494	150.6	9.051
RX1-502	153.0	9.114
RX1-511	155.8	9.135
RX1-519	158.2	9.185
RX1-527	160.6	9.071
RX1-535	163.1	9.150
RX1-544	165.8	9.053
RX1-552	168.2	8.915
RX1-560	170.7	9.002
RX1-568	173.1	9.149
RX1-576	175.6	9.217
RX1-585	178.3	8.938
RX1-593	180.7	9.171
RX1-601	183.2	9.188
RX1-617	188.1	9.089
RX1-625	190.5	9.148
RX1-634	193.2	9.077
RX1-642	195.7	8.726
RX1-708	215.8	7.325
RX1-724	220.7	9.001
RX1-732	223.1	9.198
RX1-740	225.6	8.889
RX1-748	228.0	7.717
RX1-757	230.7	8.975
RX1-773	235.6	8.880
RX1-781	238.0	9.034
RX1-790	240.8	8.881
RX1-798	243.2	9.194
RX1-801	244.1	9.340
RX1-814	248.1	9.096
RX1-816	248.7	9.366
MEAN		8.97
STANDARD DEVIATION		0.41

Table C-4.

THERMAL CONDUCTIVITY VALUES FROM WIN-1 CORE  
(SAMPLES ARE 2.680 CM IN DIAMETER)

SAMPLE IDENTIFICATION	DEPTH (METERS)	THERMAL CONDUCTIVITY MCAL/CM-SEC-°C
WN1-85	25.9	7.973
WN1-295	89.9	8.130
WN1-420	128.0	7.974
WN1-505	153.9	8.088
WN1-585	178.3	8.081
WN1-695	211.8	8.284
WN1-790	240.8	7.897
WN1-895	272.8	7.794
WN1-940	286.5	8.380
WN1-1040	317.0	8.218
WN1-1100	335.3	8.352
WN1-1240	378.0	8.025
WN1-1285	391.7	7.783
WN1-1350	411.5	7.978
WN1-1400	426.7	7.930
WN1-1482	451.7	8.119
WN1-1545	470.9	8.017
WN1-1580	481.6	8.127
WN1-1635	498.3	8.162
WN1-1660	506.0	7.553
WN1-1705	519.7	8.000
WN1-1720	524.3	7.995
WN1-1750	533.4	7.622
WN1-1780	542.5	8.769
WN1-1820	554.7	8.123
WN1-1870	570.0	8.180
MEAN		8.06
STANDARD DEVIATION		0.24

## Heat Generation

L. D. Perry and J. K. Costain

Results of heat generation determined for core samples from holes Ker 3, Win 1, and Rox 1, and for surface samples from Winnsboro, are given in Tables C-5, C-6, C-7, and C-8. The conversion factors used for heat generation are those given by Birch (1954). Rybach (1976, p. 311) has recently redefined these factors. His constants are given in Table C-9. The difference between the Birch and Rybach constants does not exceed 3% for a group of about 20 samples checked. In the future, we plan to adopt these revised constants in our calculations.

Table C-5. Heat generation data for core from drill hole Ker 3.

DEPTH INTERVAL		SAMPLE NO.	DENSITY, GM/CM3	URANIUM (U), PPM	THORIUM (TH), PPM	POTASSIUM (K), %	K2O, %	HEAT GENERATION, A X 10-13 CAL/CM3-SEC
(FEET)	(METERS)							
1.0-11	.5-3.4	K-23	(2.67)	3.15	13.77	3.83	4.60	5.15
53.5-59.7	16.3-18.2	K-24	(2.67)	3.26	15.37	4.04	4.85	5.53
41-44	12.5-13.4	K-11	(2.67)	5.65	21.33	4.09	4.90	8.03
72-82	21.9-25.0	K-31	(2.67)	4.25	35.15	4.36	5.23	9.57
102-105	31.1-32.0	K-25	(2.67)	3.16	14.84	4.19	5.03	5.42
118-128	36.0-39.0	K-21	2.67	3.14	14.29	3.98	4.78	5.27
179.5-189.9	54.7-57.9	K-32	2.65	3.85	32.92	4.40	5.28	8.95
194-204	59.1-62.2	K-22	2.66	2.85	12.61	3.94	4.73	4.79
284-294	86.6-89.6	K-33	2.69	2.25	7.37	3.79	4.55	3.50
384-394	117.0-120.1	K-34	2.65	2.46	10.11	4.17	5.00	4.18
530-540	161.5-164.6	K-35	(2.67)	2.24	10.64	4.14	4.97	4.13
670-680	204.2-207.3	K-36	2.67	8.01	9.58	4.05	4.86	7.51
790-800	240.8-243.8	K-37	2.67	2.45	12.72	4.29	5.15	4.65
924-934	281.6-284.7	K-310	(2.67)	11.66	19.68	4.12	4.94	11.47*
1110-1120	338.3-341.4	K-38	(2.67)	2.35	15.00	4.21	5.05	4.95
1160-1170	353.6-356.6	K-39	(2.67)	2.44	12.89	4.21	5.05	4.65
1210-1220	368.8-371.9	K-312	(2.67)	2.35	11.89	4.21	5.06	4.43
1260-1270	384.0-387.1	K-313	(2.67)	2.21	11.56	4.26	5.12	4.29
1304-1314	397.5-400.5	K-311	(2.67)	2.30	12.15	4.16	4.99	4.43
AVERAGE				3.69	16.28	4.14	4.97	5.69
STANDARD DEVIATION				2.35	7.99	.17	.20	1.86

C-12

(2.67) . . . ASSUMED DENSITY

. . . . . NOT USED IN COMPUTATION OF AVERAGE VALUE AND STANDARD DEVIATION

Table C-6. Heat generation data from core from drill hole Win 1 in Rion pluton.

DEPTH INTERVAL		SAMPLE NO.	DENSITY, GM/CM3	URANIUM (U), PPM	THORIUM (TH), PPM	POTASSIUM (K), %	K2O, %	HEAT GENERATION, A X 10-13 CAL/CM3-SEC
(FEET)	(METERS)							
80-86	24.4-26.2	WIN-1	(2.67)	6.54	33.31	4.18	5.02	10.63
290-296	88.4-90.2	WIN-1	(2.67)	8.14	31.42	4.11	4.93	11.28
356-357	108.5-108.8	WIN-1	(2.67)	7.69	33.00	4.68	5.61	11.40
500-506	152.4-154.2	WIN-1	(2.67)	6.83	32.65	4.06	4.88	10.67
620-626	189.0-190.8	WIN-1	(2.67)	10.64	36.75	4.44	5.33	13.80
690-696	210.3-212.1	WIN-1	(2.67)	9.32	33.13	4.24	5.09	12.33
890-896	271.2-273.1	WIN-1	(2.67)	7.72	31.05	4.16	4.99	10.97
987-993	300.3-302.7	WIN-1	(2.67)	11.18	37.43	4.34	5.20	14.23
1281-1287	390.4-392.3	WIN-1	(2.67)	6.14	33.38	4.40	5.28	10.44
1390-1396	423.7-425.5	WIN-1	(2.67)	4.49	30.06	4.79	5.75	8.95
1490-1496	454.2-456.0	WIN-1	(2.67)	5.18	28.85	4.12	4.95	9.02
1540-1546	469.4-471.2	WIN-1	(2.67)	4.86	32.11	4.34	5.21	9.42
1630-1636	496.8-498.7	WIN-1	(2.67)	7.01	32.09	4.08	4.90	10.69
1701-1707	518.5-520.3	WIN-1	(2.67)	5.14	34.44	4.33	5.19	9.99
1779-1785	542.2-544.1	WIN-1	(2.67)	6.50	32.45	4.16	4.99	10.45
1865-1871	568.5-570.3	WIN-1	(2.67)	9.30	48.97	4.46	5.35	15.05
AVERAGE				7.29	33.82	4.31	5.17	11.21
STANDARD DEVIATION				2.02	4.58	.21	.25	1.80

(2.67)...ASSUMED DENSITY

\*. . . . . NOT USED IN COMPUTATION OF AVERAGE VALUE AND STANDARD DEVIATION

C-13



Table C-7. Heat generation data for surface samples from Winnsboro pluton.

	SAMPLE NO.	DENSITY, GM/CM <sup>3</sup>	URANIUM (U), PPM	THORIUM (TH), PPM	POTASSIUM (K), %	K <sub>2</sub> O, %	HEAT GENERATION, A X 10 <sup>-13</sup> CAL/CM <sup>3</sup> -SEC	
	WINNSBORO	F6-18	(2.67)	6.14	45.90	4.43	5.31	12.30*
	WINNSBORO	F6-66	(2.67)	2.06	7.80	3.98	4.78	3.50
	WINNSBORO	S6-41	(2.67)	4.54	29.18	4.17	5.00	8.69
	WINNSBORO	S6-56	2.66	2.43	9.39	3.99	4.79	3.98
	WINNSBORO	S6-2	(2.67)	2.79	12.67	4.16	4.99	4.82
	WINNSBORO	S6-18	2.71	4.62	14.69	3.20	3.84	6.16
	WINNSBORO	S6-20	(2.67)	4.83	13.90	3.21	3.90	6.10
	WINNSBORO	S6-22	(2.67)	4.42	16.27	3.30	3.96	6.24
	WINNSBORO	S6-24	(2.67)	4.90	17.99	4.16	4.99	7.02
	WINNSBORO	S6-25	(2.67)	1.51	12.12	4.36	5.23	3.98
	WINNSBORO	S6-26	(2.67)	2.32	18.71	4.44	5.33	5.61
	WINNSBORO	S6-27	(2.67)	2.24	13.01	3.93	4.72	4.48
	WINNSBORO	S6-29	(2.67)	3.56	14.44	4.33	5.20	5.63
	WINNSBORO	S6-30	(2.67)	1.23	10.60	4.29	5.15	3.53
	AVERAGE			3.40	16.91	4.00	5.26	5.36
	STANDARD DEVIATION			1.51	9.81	.44	1.43	1.52

(2.67) . . . ASSUMED DENSITY

\* . . . . NOT IN COMPUTATION OF AVERAGE VALUE AND STANDARD DEVIATION.

C-14

Table C-8. Heat generation data for core from drill hole Rox 1.

DEPTH INTERVAL		SAMPLE NO.	DENSITY, GM/CM3	URANIUM (U), PPM	THORIUM (TH), PPM	POTASSIUM (K), %	K20, %	HEAT GENERATION, A X 10-13 CAL/CM3-SEC
(FEET)	(METERS)							
41-46	12.5-14.0	ROX-1	(2.67)	2.96	9.31	3.02	3.62	4.10
100-105	30.2-32.0	ROX-1	(2.67)	3.19	9.93	2.92	3.50	4.32
265-270	80.8-82.3	ROX-1	(2.67)	3.25	10.40	2.97	3.57	4.45
300-305	91.4-93.0	ROX-1	(2.67)	3.25	10.07	3.05	3.66	4.41
594-599	181.1-182.6	ROX-1	(2.67)	3.29	10.26	2.94	3.53	4.44
AVERAGE				3.19	9.99	2.98	3.58	4.34
STANDARD DEVIATION				.13	.42	.05	.07	.15

(2.67)... ASSUMED DENSITY

C-15

Table C-9. Revised heat generation constants,  
from Rybach (1976).

Element/decay series	A [cal/g, y] Rybach (1976)	A [cal/g, y] Birch (1954)
$U^{238}$	0.692	0.71
$U^{235}$	4.34	4.3
U (natural)	0.718	0.73
$Th^{232}$	0.193	0.20
K (natural)	$26.2 \times 10^{-6}$	$27 \times 10^{-6}$

## Relationship Between Surface Heat Generation and Surface Heat Flow

John K. Costain

Figure C-3 shows the correlation between near-surface heat generation and heat flow for drill holes Ker 3, Win 1, and Rox 1. These are the only sites for which heat flow and heat generation values are available to date. The linear relationship is remarkable and confirms our expectations that heat flow is an essential component of our targeting procedure. The equation relating heat flow,  $q$ , to heat generation,  $A$ , is found to be

$$q = 0.66 + 7.2 \times 10^5 A.$$

The values of heat flow and heat generation used are from Tables C-5 through C-8, and are listed below the plotted points in Figure C-3.

The linear relationship between heat flow and heat generation has been discussed by Birch, Roy, and Decker (1968), Lachenbruch (1968), Roy, Blackwell, and Birch (1968), and many others. Lachenbruch (1968, 1970) presented a strong geological argument for an exponential decrease with depth of the heat-producing elements. This is the only distribution for which the linear relationship would survive differential erosion.

It is surprising to observe the linear relationship in the southeast in such widely separated (450 km) plutons with such a large age span ( $\sim 275$  m.y.), in both pre- and post-metamorphic rocks. Furthermore, in spite of the relatively small sizes of the plutons, the edge effects discussed by Roy et al. (1968, p. 2) and Birch et al. (1968, p. 449) do not appear to be present, possibly because of a low contrast in heat production between any one pluton and the country rock into which it is intruded.

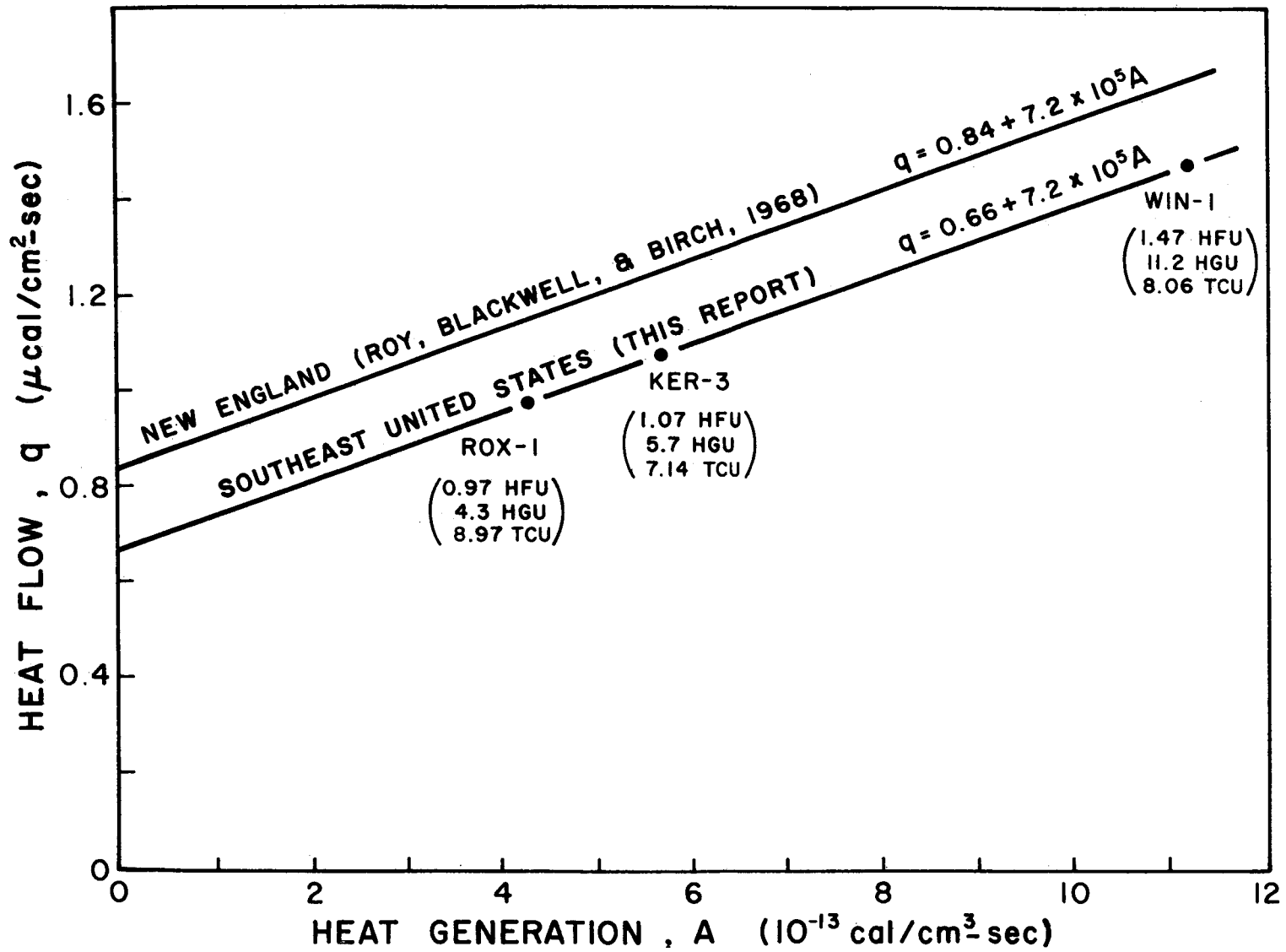


Figure C-3. Heat flow vs. heat generation in southeast United States.

The slope of the straight line in the southeast in Figure C-3 is the same as that for New England (Roy et al., 1968, p. 4) within experimental error. The intercept is lower than New England by 0.18 HFU. It is difficult to choose between possible reasons for this difference at this time. Since the slopes of the linear relationship in New England and in the southeast United States are approximately equal, then the thickness of the crustal layer of high radioactivity in the southeast must be about the same as that in New England; a different thickness would result in a different slope under the assumption that the radiogenic elements are distributed uniformly from the surface to a depth D. If the heat-producing elements decrease exponentially with depth, then the rate of change of  $A(z)$  in a vertical direction, that is, the logarithmic decrement  $D$ , must be the same in the southeast as it is in New England. We are left with the conclusion that the difference of 0.18 HFU in the intercept must be due to a locally higher contribution from the lower crust and/or mantle in the New England area. Such local variations might also exist in the southeast, and will be detected by contouring values of "reduced heat flow,"  $q^*$ , given by

$$q^* = q - DA.$$

Thus, values of reduced heat flow presumably reflect variations in heat flow from the mantle (Roy et al., 1971; Blackwell, 1971). If a heat flow province is defined as a region with the same mantle heat flow ( $q^*$ ), then within a single heat flow province there might be subareas with heat flow and heat generation lines of different slopes, but identical intercept values (Roy et al., 1971; Blackwell, 1971). In view of the

linear relation observed to date in the southeast, it seems desirable to broaden the definition of a "heat flow province" to include local variations in mantle heat flow as well as local variations in the slope of the linear relations. In the future, we must determine the heat production in country rock in selected areas as well as in the plutons themselves. If the linear relationship is to become part of our targeting procedure, then we must evaluate the importance of edge effects caused by contrasts in heat generation. Birch et al. (1968, p. 449) found that the drill sites in New England in the New Hampshire Plutonic Series were "surrounded for considerable distances by rocks having on the average about the same radioactivity as the granites in which the measurements were made. . . ."

As discussed in detail by Lachenbruch (1968, 1970), any vertical distribution of heat-producing elements will result in a linear relationship between near-surface heat flow and near-surface heat generation as long as

$$\int_0^{\infty} A(z') dz' = D A_0$$

where D is the (constant) slope of the straight line relating heat flow to heat generation,  $A_0$  is the surface heat generation, and  $A(z)$  is the (arbitrary) distribution of heat-producing elements with depth  $z$ ; however, if the relationship is to survive differential erosion, then we must have (Lachenbruch, 1968, p. 6981)

$$\int_z^{\infty} A(z') dz' = D A(z) \quad z \geq 0.$$

The only distribution,  $A(z)$ , for which this is possible is

$$A(z) = A_0 e^{-z/D}.$$

Albarede (1975) discussed a theoretical model based on the mathematics of zone melting (Pfann, 1952) which supports Lachenbruch's proposed exponential distribution.

Values of heat generation from basement rocks beneath sediments of the Atlantic Coastal Plain will be necessary to delineate regions of higher reduced heat flow. We should expect to see scatter in the linear relationship where values of reduced heat flow change. Roy et al. (1971) and Blackwell (1971, p. 172) point out that transition zones between regions of different mantle heat flow are generally narrow compared with the dimensions of regions of uniform mantle heat flow.

Jaeger (1970) found a linear relationship for the western portion of the Australian shield (using three points) of the form

$$q = 0.64 + 4.5 \times 10^5 A.$$

Thus the mantle heat flow is in good agreement with that inferred for the southeastern United States. Slack (1974) deduced a mantle heat flow value of 0.68 HFU for craton and shield areas, again in good agreement with the data observed to date in the southeastern United States.

While it may be premature to draw too many conclusions based on the limited data available in the southeast United States, the results to date are encouraging for the following reasons:

- 1) The linear relation between heat flow and heat generation appears to hold in the southeastern United States.
- 2) The inferred mantle heat flow is similar to that proposed elsewhere for craton and shield areas.



- 3) The slope of the linear relation is the same as that for New England.
- 4) The mantle heat flow for New England may therefore be anomalously high and of relatively "local" extent, and should not be used to define a general relation between heat flow and heat generation for the entire eastern United States.
- 5) Transition zones between areas of different "reduced heat flow" are relatively narrow.
- 6) Similar regions of anomalously high mantle heat flow may exist in the southeastern United States.

## Partial Confirmation of Radiogenic Model

John K. Costain

Figure C-4 shows the temperature profile and geothermal gradient obtained by VPI & SU in an existing hole at Stumpy Point, North Carolina. The hole was drilled by the Rapp Oil Company in 1970 in sediments of the Atlantic Coastal Plain to a total depth of 1.66 km (5440 ft.) The location of the hole is shown in Figure C-5. The least-squares geothermal gradient over the interval 302 m to 1349 m is  $37.4^{\circ}\text{C}/\text{Km}$  ( $\sim 2^{\circ}\text{F}/100'$ ). The hole was blocked at 1.35 km.

The hole is located on the flank of a broad gravity low. If we assume a mean conductivity of Coastal Plain sediments of  $4.2 \text{ mcal}/\text{cm}\text{-sec-}^{\circ}\text{C}$  (USGS Open-file Report 76-148), a sediment thickness of 2.3 km (Brown and Miller, 1972, Plate 5), a conductivity of granitic rocks beneath the Coastal Plain sediments of  $7 \text{ mcal}/\text{cm}\text{-sec-}^{\circ}\text{C}$ , and a mean annual surface temperature of  $16.3^{\circ}\text{C}$  (VPI&SU-5103-2, p. 108, Fig. D-10), then these parameters predict a heat generation of 12.5 HGU in the (assumed) burial granitic plutonic rocks. This is not an unreasonable heat generation based on values we have observed in the Piedmont. If the heat generation of basement rocks is assumed to be, say 4 HGU, then the gradient in the overlying sediments should be only  $23^{\circ}\text{C}/\text{Km}$ . If the heat generation is 4 HGU, then the conductivity of the overlying sediments would have to be about 2.6 TCU in order to establish the observed gradient of about  $37^{\circ}\text{C}/\text{Km}$ . This conductivity seems unreasonably low.

The hole at Stumpy Point therefore appears to provide the first partial confirmation of our theoretical model of buried radiogenic rocks beneath a sedimentary insulator. Assuming the thermal conductivity

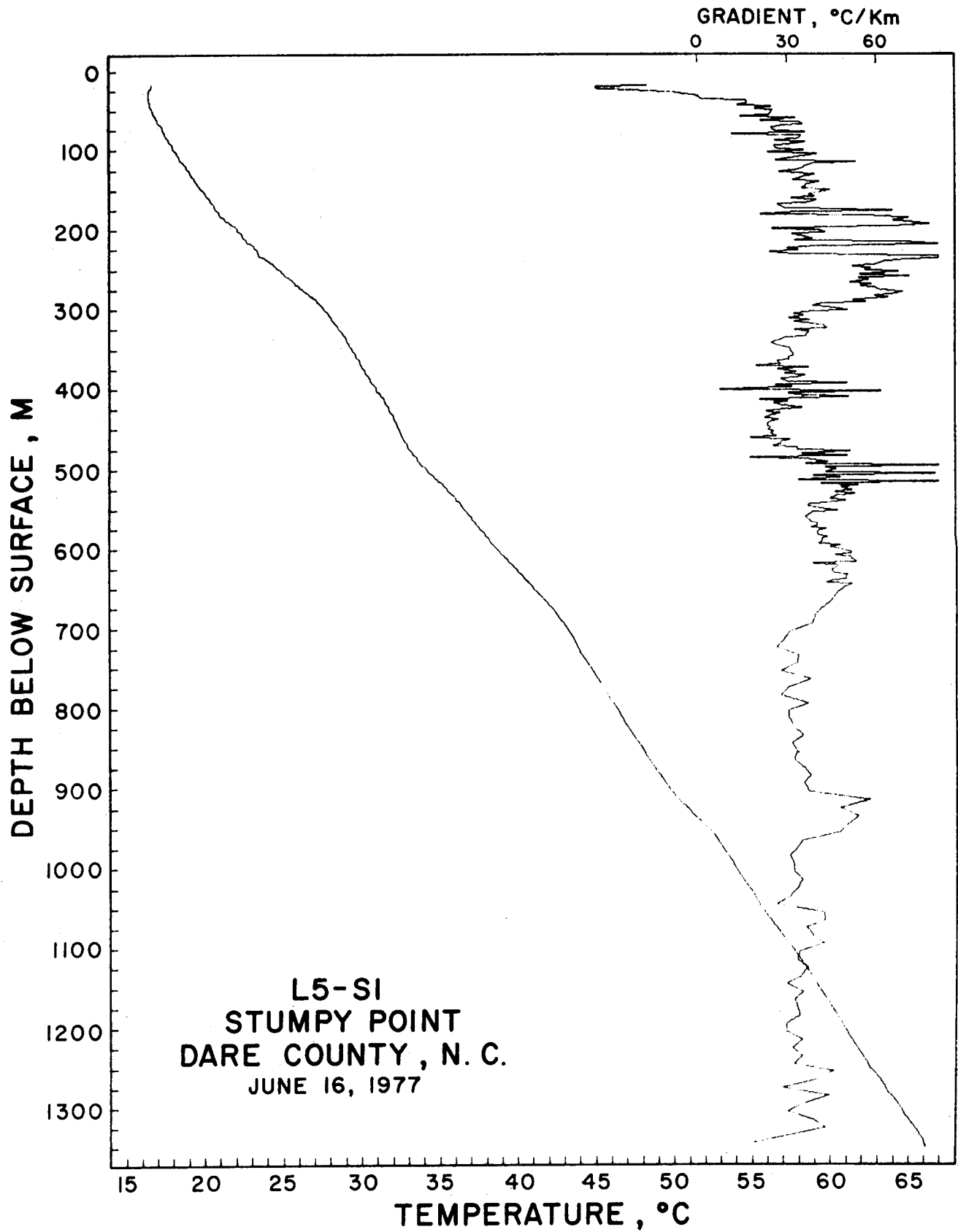


Figure C-4. Temperature profile and gradient at Stumpy Point, North Carolina.

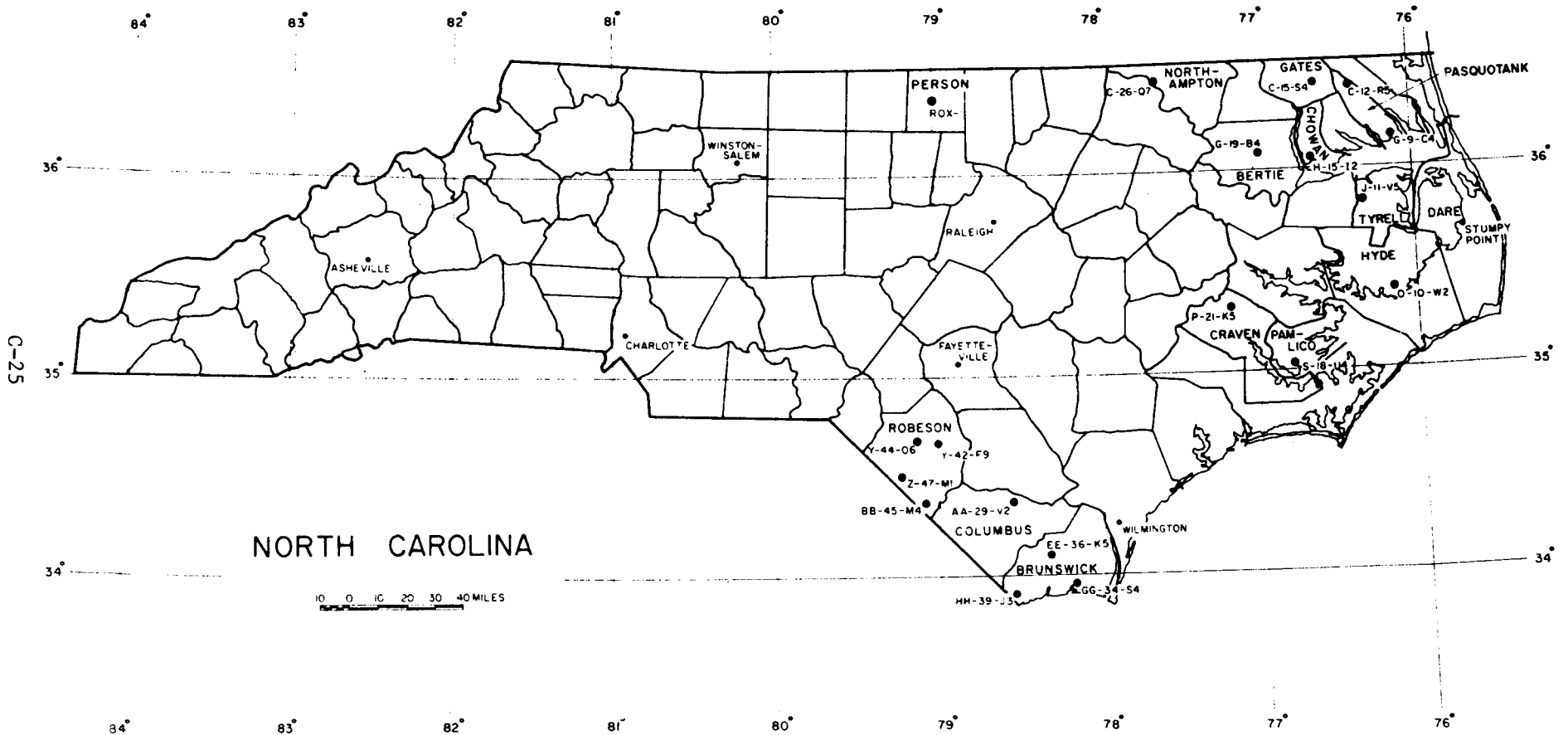


Figure C-5. Locations of existing wells logged to date in North Carolina.

remains approximately 4.2 TCU to the base of the sediments at 2.3 km, the bottomhole temperature would be 102°C. If the conductivity increases to a mean of 4.5 TCU, the predicted bottomhole temperature is 96°C. If it decreases to 4 TCU, the predicted bottomhole temperature is 106°C.

As discussed earlier in this report, an important factor in predicting subsurface temperature is the determination of the contrast in heat generation between radiogenic plutons and the country rock into which they have been intruded. Birch et al. (1968) found little contrast between the heat generation of the intrusive rocks of the New Hampshire Magma Series and that of the surrounding country rock, the Littleton Formation. On the other hand, corrections were necessary for the finite size of the Conway Granite of the White Mountain Magma Series since the Conway Granite is approximately twice as radioactive as the surrounding country rock, and the drilling sites were within less than 5 km of the mapped contacts with less radioactive formations (Birch et al., 1968, p. 449). Consequently, the heat flow near the margins is less than it would be at stations nearer the center of the intrusive. Their corrections amounted to approximately 10%, but the corrections could be considerably greater (Roy et al., 1968, p. 2). Since the hole at Stumpy Point is located on the flank of a broad gravity low, higher values of heat flow and/or geothermal gradients might be found at sites more centrally located with respect to the anomaly.

## Interpretation of Gravity Data

J. A. Dunbar

An attempt is being made to locate and determine the general sizes and shapes of granitic bodies concealed beneath the coastal plain sediments. As a first step, the amplitudes and shapes of gravity anomalies on the Coastal Plain will be compared to the gravity expressions of the large granitic bodies exposed in the Piedmont. Since similar bodies produce similar gravity expressions, this comparison should identify areas which merit further investigation. Before a valid comparison can be made, it is necessary to account for the effect on the gravitational field of the thickening wedge of coastal plain sediments.

A preliminary gravity model of the Norfolk, Virginia area was used to evaluate the effect of increasing the depth of burial of a low density body on the gravity anomaly. The model is a single homogeneous body with a density contrast of  $-0.2 \text{ g/cm}^3$ , the top of which is 0.6 km below ground surface (VPI&SU-5103-3, p. C-29). Figure C-6A shows the gravity effect of the same body but with its top at ground surface. This gravity low differs only slightly in shape and amplitude from the gravity anomaly produced by the original model, shown in Figure C-6B. The gravity effect of the body with its top at 1.6, 2.6, 3.6 and 4.6 km below ground surface is shown in Figure C-6C, D, E and F, respectively. Since lowering the top of the model is equivalent to an upward continuation of the field, there is a rapid attenuation of high-frequency harmonics in the gravitational field of the body as its depth of burial is increased. As a result, the "half-width" distance of all of the gravity anomalies

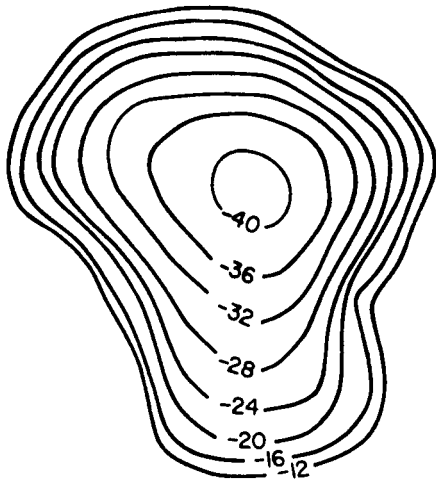
shown in Figure C-6 is essentially the same. The maximum amplitude of the gravity anomalies are, however, greatly effected by changes in depth of burial.

A gravity anomaly over a low density body similar to that which causes the Norfolk gravity low would be expected to have a similar "half-width" distance even if it were buried beneath an additional 4 km of coastal plain sediments. The maximum amplitude of this gravity anomaly would be expected to be about 3 mgal lower for each of the first four additional kilometers of burial.

Once areas of interest are defined, the effects of the sediments can be removed by computing "best-fit" polynomials of one or two degrees of freedom and subtracting them from the Bouguer gravity field.

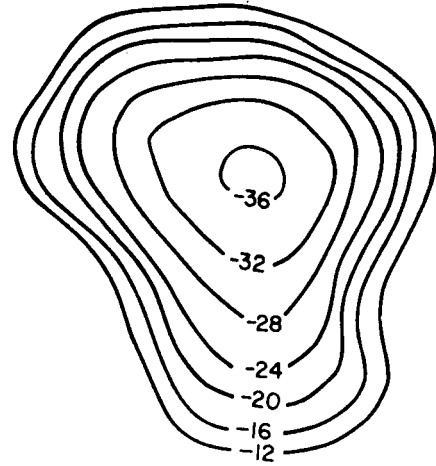
In the Norfolk, Virginia area, this procedure defined an essentially plane regional gradient of  $-0.13$  mgal/km trending toward the Atlantic coast. Gravity models based on well data (Brown and Miller, 1972) and density values (GSA Special Paper No. 36, 1942) indicate that the increase in the thickness of the Coastal Plain sediments toward the coast could account for the regional gradient.

A



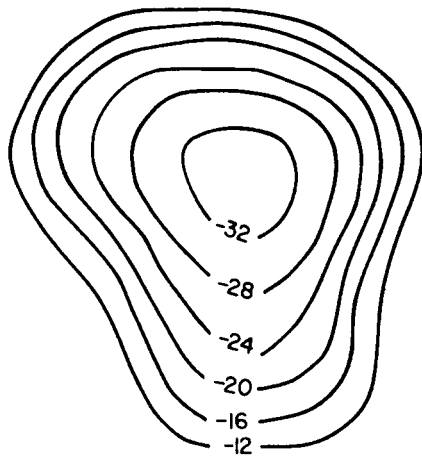
TOP OF PLUTON AT SURFACE

B



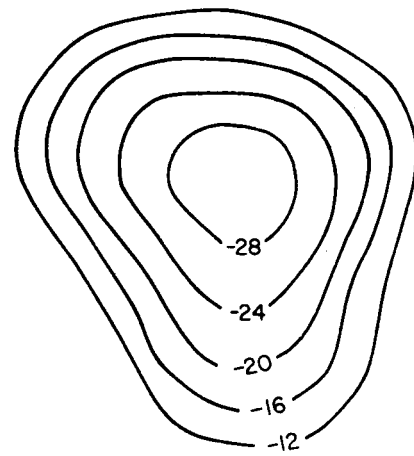
TOP OF PLUTON AT 0.6km  
(DEPTH TO BASEMENT)

C



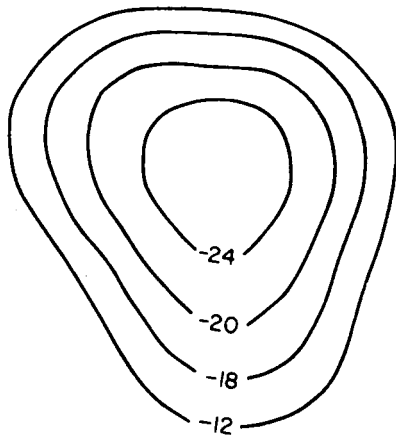
TOP OF PLUTON AT 1.6km

D



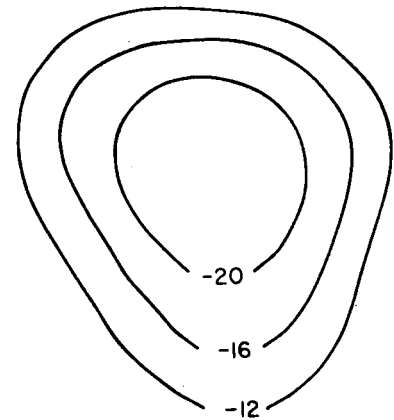
TOP OF PLUTON AT 2.6km

E



TOP OF PLUTON AT 3.6km

F



TOP OF PLUTON AT 4.6km

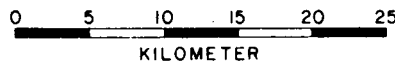
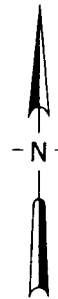


Figure C-6. Upward continuation of gravitational field of granitic pluton from surface (A) to top at 4.6 km (F).



## References

- Albarede, F., 1975, The heat flow/heat generation relationship: An interaction model of fluids with cooling intrusions: *Earth Planet. Sci. Lett.* 27, 73-78.
- Birch, F., 1954, Heat from radioactivity: *in* *Nuclear Geology*, H. Faul, ed., John Wiley & Sons, New York, p. 148-174.
- Birch, F., R. F. Roy, and E. R. Decker, 1968, Heat flow and thermal history in New England and New York: *in* *Studies of Appalachian Geology*, E-an Zen, W. S. White, J. B. Hadley, and J. B. Thompson, Jr., eds., Northern and Maritime, Interscience, New York, p. 437-451.
- Blackwell, D. D., 1971, The thermal structure of the continental crust: *in* *The Structure and Physical Properties of the Earth's Crust*, Am. Geophys. Union, Monograph 14.
- Bullard, E. C., 1939, Heat flow in South Africa: *Proc. Royal Soc. Ser. A* 173, 474.
- Costain, J. K., and P. M. Wright, 1973, Heat flow at Spor Mountain, Jordan Valley, Bingham, and La Sal, Utah: *J. Geophys. Res.* 78, 8687-8698.
- Jaeger, J. C., 1970, Heat flow and radioactivity in Australia: *Earth Planet. Sci. Lett.* 81, 285-292.
- Lachenbruch, A. H., 1968, Preliminary geothermal model for the Sierra Nevada: *J. Geophys. Res.* 73, 6977-6989.
- Lachenbruch, A. H., 1970, Crustal temperature and heat production: Implications of the linear heat flow relation: *J. Geophys. Res.* 75, 3921-3300.
- Pfann, W. G., 1952, Principles of zone melting: *J. Metals, Trans. AIME*, 747-753.
- Reiter, M. A., and J. K. Costain, 1973, Heat flow in southwestern Virginia: *J. Geophys. Res.* 78, 1323-1333.
- Roy, R. F., D. D. Blackwell, and F. Birch, 1968, Heat generation of plutonic rocks and continental heat flow provinces: *Earth Planet. Sci. Lett.* 5, 1-12.
- Roy, R. F., D. D. Blackwell, and E. R. Decker, 1971, Continental heat flow: *in* *Nature of the Solid Earth*, E. C. Robertson, ed., McGraw-Hill, New York.
- Rybach, L., 1976, Radioactive heat production in rocks and its relation to other petrophysical properties: *Pageophys.* 114, 309-317.
- Slack, P. B., 1974, Variance of terrestrial heat flow between the North American Craton and the Canadian Shield: *Bull. Geol. Soc. Am.* 85, 519-522.